

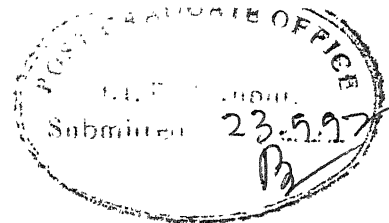
COMPUTATIONAL ANALYSIS OF HEAT AND MASS TRANSFER IN DOUBLE - EFFECT SOLAR STILL

A Thesis Submitted
in Partial Fulfilment of the Requirements
for the Degree of
MASTER OF TECHNOLOGY

by
RAJEEV SABHARWAL

to the
DEPARTMENT OF MECHANICAL ENGINEERING
INDIAN INSTITUTE OF TECHNOLOGY KANPUR

SEPTEMBER 1992



CERTIFICATE

Certified that the thesis entitled "COMPUTATIONAL ANALYSIS OF HEAT AND MASS TRANSFER IN- DOUBLE-EFFECT SOLAR STILL" by Mr. Rajeev Sabharwal has been carried out under our supervision and that this work has not been submitted elsewhere for the award of a degree.

Dr. P.N.KAUL
Assistant Professor

Department of Mechanical Engineering
Indian Institute of Technology
Kanpur-208016

Dr. H.C.AGRawal
Professor

Department of Mechanical Engineering
Indian Institute of Technology
Kanpur-208016

ACKNOWLEDGEMENTS

I wish to express my deep sense of gratitude and sincere regards to Drs. H.C.Agrawal and P.N. Kaul for their invaluable guidance and constant encouragement in the successful completion of this work.

I express my appreciation and indebtedness to my friends M/s Shreesh Jadav, A.K. Singh, Vivek Kumar, Anurag Goyal, Himanshu Tewari, Niraj Srivastava, Varshni and others who apart from making my stay at Kanpur very pleasant and memorable also helped me from time to time in many ways.

Rajeev Sabharwal

24 FEB 1993

CENTRAL INTELLIGENCE

AGENCY FILE NO.
114835

ME-1992-M-SAB-COM

CONTENTS

	<u>PAGE</u>
CERTIFICATE	i
ACKNOWLEDGEMENTS	ii
LIST OF CONTENTS	iii
LIST OF FIGURES	v
NOMENCLATURE	vi
ABSTRACT	ix
CHAPTER 1	INTRODUCTION
1.1	Energy: Crisis and renewable source
1.2	Solar energy
1.3	Importance of solar still
1.4	Review of previous work
1.5	Analytical approaches
1.5.1	Single Basin Solar Still
1.5.2	Simple Multiple Wick Solar Still
1.5.3	Double Basin Solar Still
1.6	Present work
CHAPTER 2	MATHEMATICAL MODEL
2.1	Development of the model
2.2	Attenuation of solar radiation in a water layer
2.3	Absorptivity and transmittance of a water layer on a glass plate
2.4	Governing equations
2.4.1	Energy balance for the top glass cover
2.4.2	Energy balance for the intermediate glass plate
2.4.3.	Energy balance for the absorbing plate
2.4.4	Balancing of evaporation rates
2.5	Numerical solution
CHAPTER 3	RESULTS AND CONCLUSIONS
3.1	Input data
3.2	Discussions of results

3.3	Conclusions	44
3.4	Suggestions for future work	48
REFERENCES		49
APPENDIX A		51
APPENDIX B		55

LIST OF FIGURES

FIGURE	TITLE	PAGE
1.1	Average solar radiation for ESCAP countries	3
1.2	Single Basin Solar Still	8
1.3	Simple multiple wick solar still	11
1.4	Double basin solar still	13
2.1	Schematic diagram of Double-Effect solar still	17
2.2	Fraction of incident energy remaining after passing through a thickness z	22
2.3	Water layers on the glass plate	23
2.4	Energy Fluxes in Double-Effect solar still	25
3.1	Average daily values of global solar radiation for New Delhi	33
3.2	Variation of temperature of the cover, the intermediate glass plate and the absorber plate	34
3.3	Distillate outputs from the first and second effects	36
3.4	Comparison of distillate outputs of the single and double-effect stills	37
3.5	Comparison of efficiencies of single and double-effect stills	38
3.6a	Hourly variation of global solar radiation	40
3.6b	Hourly variation of temperatures of glass cover, intermediate glass plate and absorber plate	41
3.6c	Hourly variation of distillate output	42
3.7	Effect of ambient air velocity on distillate output	43
3.8	Effect of inlet water temperature on distillate output	45
3.9	Effect of operating pressure on distillate output	46
3.10	Effect of mass flow rate in lower stage on distillate output	47

NOMENCLATURE

A_b	surface area of glass plate between weirs, m^2
A_{we}	surface area of weirs, m^2
A_w	surface area of water layer between two weirs, m^2
a, b	constants defined in eq.(3) and shown in Table (2.2)
c	constant(in cm.) defined in eq(3) and shown in Table (2.2)
$C_{pa}; C_{pw}$	Heat capacity of dry air; water , J/kg-K
$D_1; D_2$	Net distilled water production rate , Kg/m^2-hr
$F_c; F_2$	Modified Factor for glass cover; intermediate glass plate
$f(z)$	Fraction of incident energy remaining after passing through a thickness z
g	Gravitational acceleration ($9.81 m/s^2$)
$H_1; H_2$	Chamber height of the first; second effect , m
h_1	Convective heat transfer coefficient between absorber and glass plates, W/m^2-K
$h_{weg}; h_{wgc}$	Convective heat transfer coefficient the glass cover and weirs; between the glass cover and the surface of water layer , W/m^2-K
h_a	Convective heat transfer coefficient between the glass cover and air, W/m^2-K
I_0	Solar radiation incident per unit surface area of cover, W/m^2
K_a	Thermal conductivity of air , $W/m-K$
$L; l$	Distance between two weirs; length of the still, m
\dot{m}_{a2}	Mass of air transferred per unit area per unit time, Kg/m^2-s
$M_a; M_w$	Molecular weight of dry air; water

$M_1; M_2$	Mass of inlet water in the first; second effect, (Kg/m ² -hr)
Nu_1, Nu_{wgc}, Nu_{weg}	Nusselt numbers
Pr	Prandtl number
$P_{s,1}; P_{s,2}; P_{s,c}$	Vapor pressure of water at $T_1; T_2; T_c$, mm of Hg
P_t	Total pressure, mm of Hg
$Q_{c1}; Q_{r1}$	Convective; Radiative heat flux from the absorbing plate to the intermediate glass plate, W/m ²
Q_{c2}, Q_{r2}	Convective; Radiative heat flux from the intermediate glass plate to the glass cover, W/m ²
$Q_{ca}; Q_{ra}$	Convective; Radiative heat flux from the glass cover to the ambient, W/m ²
RA	Rayleigh number
T	Absolute temperature, K
$T_1; T_2; T_c$	Temperature of the absorbing plate; intermediate glass plate; glass cover, K
$T_a; T_i$	Temperature of the ambient; the inlet water, K
V	Wind speed in atmosphere, m/s
W	Width of solar still, m
W_c	Absolute humidity of air at the condensing surface of the cover
$W_{s,2}$	Absolute humidity of air saturated with water vapor at T_2
y	Axis parallel to the plate surface
z	Depth of water layer, cm

GREEK LETTERS

α	Thermal diffusivity of air, m ² /s
$\alpha_g; \alpha_w$	Absorptivity of the glass cover; the water layer

α_b	Absorptivity of basin liner
β	Thermal expansion coefficient of air, K^{-1}
$\epsilon_g; \epsilon_w$	Emissivity of glass cover; the water surface
λ	Latent heat of water, J/Kg
ρ_a	Stefan-Boltzmann constant ($5.6697 \times 10^{-8} \text{ W/m}^2 \text{ K}^4$)
$\vartheta(x,t)$	Temperature distribution, $^{\circ}\text{C}$
$\tau_g; \tau_w$	Transmittance of the glass cover; water surface
τ_1	$(1-R_g)\alpha_g$
τ_2	$(1-R_g)(1-\alpha_g)\alpha_w$
τ_3	$(1-R_g)(1-\alpha_g)(1-\alpha_w)\alpha_b$
ν_a	Dynamic viscosity of air, m^2/s
μ_a	Absolute viscosity of air, N-s/m^2
η	Efficiency

ABSTRACT

A theoretical model for the heat and mass transfer in a double-effect solar still has been developed. An algorithm is also presented to determine the thermal behaviour of the still. The model developed incorporates a detailed representation of the losses from the surface of the still and uses hourly and yearly meteorological data for Delhi to predict its performance. The special features of the solar still investigated comprise a thin film of water flowing continuously over the absorber plate constituting the first stage of the still and another stream of saline water flowing over the top serrated surface of the transparent plate. This exposes a larger water surface to insolation as compared to a simple basin type still of the same dimensions and thus constitutes the second stage of the still. Besides, the entire unit is kept at optimum tilt from the horizontal to receive maximum amount of solar radiation. The effects of various design, climatic and operational parameters on the performance of the still has also been studied. The assumption that the air is saturated at all points inside the still has been relaxed to bring the model as close as possible to the reality in practice. It is seen that the double-effect solar still is 35 to 40 percent more efficient than the single-effect still in distillate production. Besides, the efficiency of the still can be enhanced by varying the operational and design parameters.

CHAPTER - 1

INTRODUCTION

1.1 ENERGY: CRISIS AND RENEWABLE SOURCES

It is a well known fact that energy represents the source of activities of human beings and nature. It was the discovery of new sources of energy like coal, petroleum products and hydroelectricity which provided a tremendous impetus to the industrialization and it was the quantitative availability of these energy resources which mainly contributed to the pace of development of the now industrialized nations. But, unfortunately, the pattern of consumption in the first half of this century has been, rather, wasteful as no attempt seems to have been made to conserve energy with a foresight into the future.

The oil embargo of the early seventies shifted the focus to the renewable sources of energy. There is hardly any disagreement on the importance of harnessing renewable sources of energy, especially solar energy in the immediate future. At a time when world is becoming more and more aware of the problems of increased pollution and mounting cost, this clean source of energy deserves a serious attention in the world energy plans.

1.2 SOLAR ENERGY

Sun [2], the source of solar energy is a sphere of internally hot gaseous matter. The rate of energy generation, due to fusion reactions in the sun is around 12×10^{12} Q (1 Q = 10^{21} JOULES). Out of this only a very small portion, around 5300 Q enters the Earth's atmosphere. Even this small fraction is huge compared to

the total world energy consumption of 0.3 Q per annum. However, all this energy, that enters the atmosphere, does not reach the surface of the earth. While at a point outside the atmosphere, the energy intensity is 1353 W/m^2 , the average amount received on the earth's surface is just about 690 W/m^2 . This value may vary with location, seasons (i.e. day of the year) and the time of the day.

It is observed that the sites lying between the latitudes of 30° North and South of the equator have sufficiently high solar intensities even during the winter months. India with its extreme latitudes of 8° and 32° North is fortunately very well placed for solar energy utilization. Actual solar radiation measurements in various ESCAP (Economic and Social Commission for Asia and the Pacific) countries have been used to produce charts of total solar radiation per unit area per unit time. The attached chart of Figure 1.1 shows that India receives the maximum solar radiation which for India works out to be 2100 KW-h per year per square meter area.

However, the main problems being faced by the solar energy utilization are its low intensities requiring large collector areas, low overall system efficiencies and the need of auxiliary equipment due to its intermittent availability.

1.3 IMPORTANCE OF SOLAR STILL

Water is a basic necessity of man along with food and air; the importance of supplying hygienic potable/ freshwater (containing less than or about 500 parts per million of salt) can hardly be over stressed. Man has been dependent on rivers, lakes and underground water reservoirs for fresh water requirements in

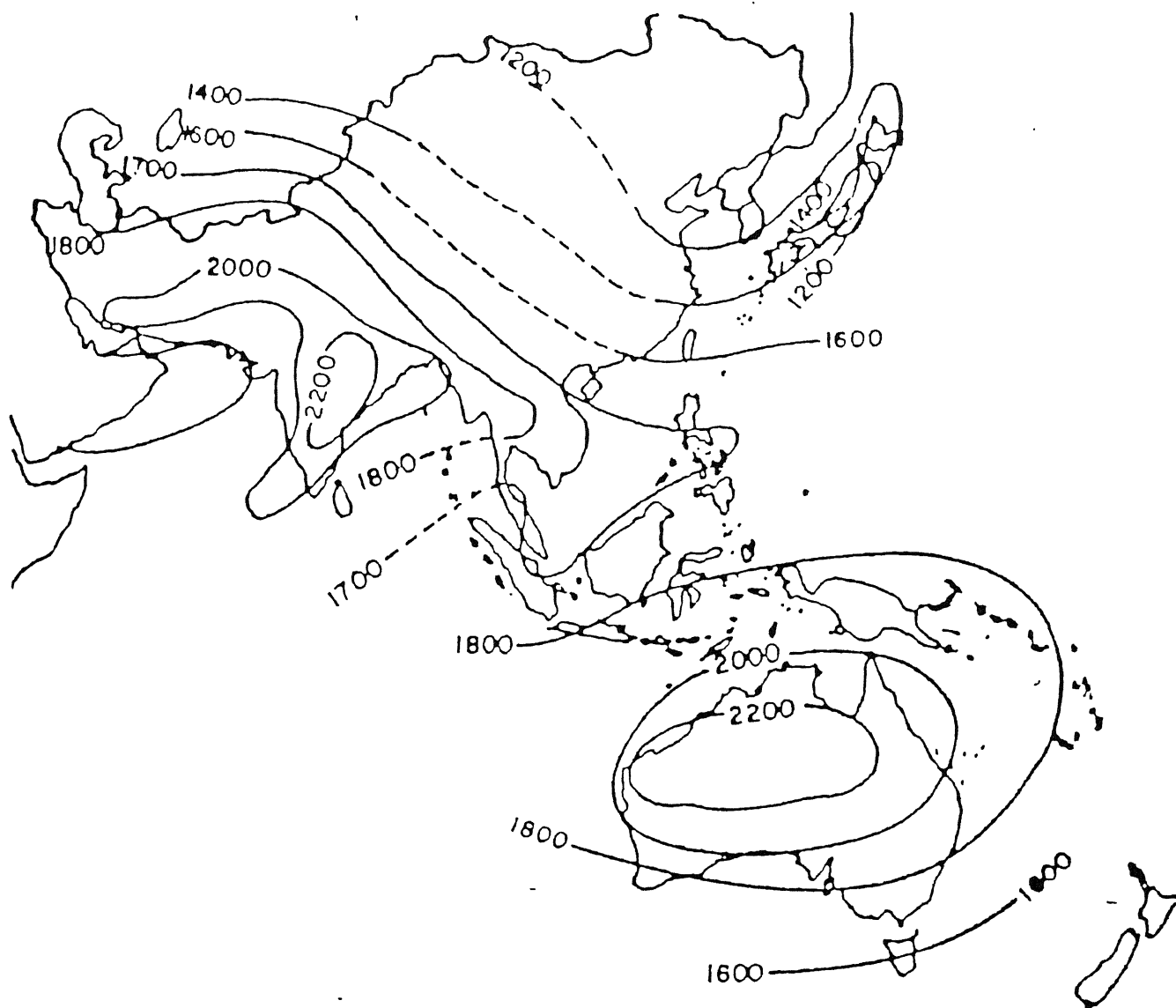


Fig.1.1 Average solar radiation (in KWh per year per square meter area) for ESCAP countries

domestic life, agriculture and industry. However, use of water from such resources is not always possible or desirable on account of the presence of large amount of salts and harmful organisms. Besides this there are several regions on the surface of this earth e.g the deserts, which have inhospitable climatic conditions and have only brackish water resources . In such places fresh water will have to be provided not only for domestic use, but also for agricultural needs.

The only inexhaustible sources of water are the oceans. Besides, there are also several, hitherto unused, big lakes, inland seas and underground natural reservoirs containing salt/brackish water. The chief drawback, obviously, is the very large salinity of such water. One of the very attractive schemes to tackle the problem of water shortage is the distillation of such water resulting in desalination. The conventional distillation processes are not only energy intensive but are also uneconomical for not too large demands of fresh water. However the developments in the use of solar energy have demonstrated that it is ideally suited for desalination, when the demand for fresh water is not too large. The rapid escalation in the cost of the fuels has made the solar alternative more attractive; in certain remote areas, this may be the only alternative. The least that can be said of solar distillation (distillation of saline water by use of solar energy) is that it is a viable option for providing hygienic potable water for a single house or a small community in most places of the earth. Further, the development of green-houses has resulted in minimizing the water requirements for carrying on agriculture on a small scale; thus solar desalination can support

small scale agriculture in regions having only brackish water sources.

1.4 REVIEW OF PREVIOUS WORK

Solar distillation has been in practice for a long time. The earliest documented work is that of the Arab alchemists in 1551. In their historical review on desalination of water, NEBBIA and MENOZZI in 1966 [29] mention the work of DELLA PORTA which he published in 1589.

The great French chemist LAVOISIER in 1862 used large glass lenses, mounted on elaborate supporting structures, to concentrate solar energy on the contents of distillation flasks. The use of Silver or Aluminum coated glass reflectors to concentrate solar energy for distillation purposes has also been described by MOUCHOT [26]. Thus it appears that in 19th century scientists were familiar with harnessing solar energy for distillation not only by direct exposure to the sun but also by concentrating sun's rays by means of mirrors and lenses.

The conventional solar distillation apparatus (commonly known as solar still), was first designed and fabricated in 1872 near Las Salinas in Northern Chile by CARLOS WILSON. This was a large basin type solar still, meant for supplying fresh water to a nitrate mining community .

No work on solar distillation seems to have been published after 1880's till the end of the First world war. With the renewal of interest in solar distillation, several types of devices have been described, e.g. roof type, tilted wick, inclined tray etc. Use of metal coated reflectors as solar concentrators for application in solar distillation has been described by KAUSCH;

PASTEUR [30] in 1928 also used several concentrators to focus solar rays onto a copper boiler containing water.

ABBOT in 1938[27] used cylindrical parabolic reflectors (aluminum coated surface) to focus solar energy onto evacuated tubes containing water. He also devised a clock-work arrangement to track the motion of the sun.

During the second world war, MARIA TELKES developed air inflated plastic stills for the U.S. Navy and Air Force for use in emergency life-rafts.

The next stage in the development of solar stills was to improve the operating efficiencies of the various type of solar distillation devices. Forced air circulation was tried within stills to enhance the vapor condensation rate. Several investigators have attempted to make use of latent heat of vaporization released by the condensing vapor in either designing multiple-effect systems or for preheating the brine to increase the output of the stills. Several large scale distillation plants and integrated schemes for combining electric power generation and desalination of water have also been suggested as a way of improving the overall operating efficiency of the plant.

The basin type solar still (also called as the greenhouse type , roof type , simple or conventional type) is in the most advanced stage of development. Several workers have investigated the effect of climatic, operational and design parameters on the performance of such a still. In attempts to improve the efficiency of distillation process, a large number of models for solar stills have also been suggested by various investigators.

1.5 ANALYTICAL APPROACHES

There have been number of attempts to solve the heat and mass transfer equations, applied to solar stills, analytically and predict their performance. A few important contributions in this direction are discussed below:

1.5.1 SINGLE BASIN SOLAR STILL

Cooper[25] and Frick [28] considered the periodicity of solar insolation and ambient temperature in the analysis of the solar still. However, the major drawback in their analysis has been that in the Fourier expansion of the periodic quantities only the fundamental harmonics have been retained. Also, they considered in their analyses an ideal solar still with many assumptions. Nayak et al.[12] presented the following analysis to predict the performance of a solar still with more general periodic behaviour of solar insolation and ambient temperature. A schematic sketch of the still analyzed by him is shown in Fig. 1.2 . The energy balance conditions at the top cover, saline water and the absorbing surface were be written as

$$M_g \times dT_g / dt = \tau_g \times H_s + q_{rw} + q_{cw} + q_{ew} - q_a \quad \dots(1)$$

$$M_w \times dT_w / dt = \tau_2 \times H_s + q_w - q_{cw} - q_{rw} - q_{ew} \quad \dots(2)$$

$$\tau_3 \times H_s = q_w + q_{ins} \quad \dots(3)$$

where

$$\begin{aligned} q_{cw} &= \text{Convective heat transfer from water to glass cover} \\ &= h_{cw} \times (T_w - T_g) \quad \dots(4) \end{aligned}$$

$$\begin{aligned} q_{ew} &= \text{Evaporative heat transfer from water to glass cover} \\ &= h_{eff} \times (T_w - T_g) \quad \dots(5) \end{aligned}$$

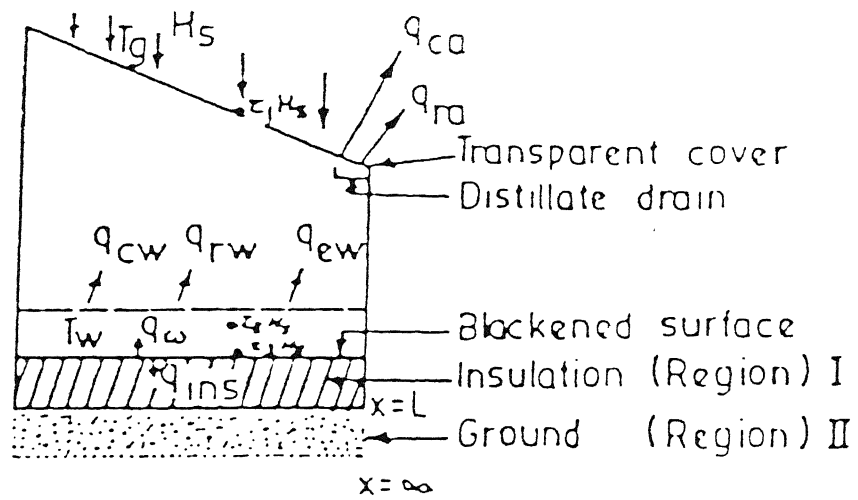


Fig.1.2 Single Basin Solar Still

$$\begin{aligned}
 q_{rw} &= \text{Radiative heat transfer from water to glass cover} \\
 &= h_{rw} \times (T_w - T_g) \quad \dots(6)
 \end{aligned}$$

$$\begin{aligned}
 q_a &= \text{Total heat loss from cover to ambient} \\
 &= h_2 \times (T_g - T_a) \quad \dots(7)
 \end{aligned}$$

Energy transferred from the absorbing surface to the saline water is written as

$$q_w = h_3 \times [\vartheta_1|_{x=0} - T_w] \quad \dots(8)$$

while the loss to the insulation from the absorbing surface is given by

$$q_{ins} = -K_1 (\partial\vartheta/\partial x)|_{x=0}$$

where $\vartheta_1(x,t)$ is the temperature distribution below the absorbing surface. The temperature distribution $\vartheta(x,t)$ in the insulation and ground is governed by the heat conduction equation

$$\rho_j C_j (\partial\vartheta/\partial t) = K_j (\partial^2\vartheta/\partial x^2) \quad j=1,2 \quad \dots(9)$$

subject to the boundary conditions

$$\vartheta_1(x=L,t) = \vartheta_2(x=L,t) \quad \dots(10)$$

$$-K_1 (\partial\vartheta_1/\partial x)|_{x=L} = -K_2 (\partial\vartheta_2/\partial x)|_{x=L} \quad \dots(11)$$

and

$$\vartheta_2(x,t) \text{ is finite for } x \rightarrow \infty \quad \dots(12)$$

The solar intensity and ambient air temperature were considered to be periodic in time and Fourier analyzed in the form

$$H_s = a_0 + \text{Re} \sum_n A_n \exp [i(n\omega t - \sigma_n)] \quad \dots(13)$$

and

$$T_a = b_0 + \text{Re} \sum_n B_n \exp [i(n\omega t - \phi_n)] \quad \dots(14)$$

$$\text{where } \omega = 2\pi/(24 \times 60 \times 60) \text{ sec}^{-1}$$

The following periodic solutions were assumed.

$$\begin{aligned}
 \vartheta_1(x,t) = & A_1 x + B_1 + \text{Re} \sum_n \{C_{1n} \exp(-\beta_{1n} x) + D_{1n} \exp(\beta_{1n} x)\} \exp(in\omega t) \\
 & \text{for } 0 \leq x \leq L
 \end{aligned}$$

$$\phi_2(x,t) = B_2 + \operatorname{Re} \sum_n C_{2n} \exp(in\omega t - \beta_{2n}x) \quad \text{for } x \geq L$$

$$T_g(t) = g_0 + \operatorname{Re} \sum_n g_n \exp(in\omega t)$$

and

$$T_w(t) = H_0 + \operatorname{Re} \sum_n H_n \exp(in\omega t)$$

where

$$\beta_{1n} = (n)^{1/2} \alpha_1 (1 + i)$$

$$\beta_{2n} = (n)^{1/2} \alpha_2 (1 + i)$$

$$\alpha_j = (\omega \rho_j C_j / 2K_j)^{1/2} \quad j = 1, 2$$

The constants A_1 , B_1 , A_2 , B_2 , C_{1n} , g_0 , g_n , H_0 and H_n were determined from equations given above and the exact solutions obtained.

1.5.2 SIMPLE MULTIPLE WICK SOLAR STILL

Kumar and Sodha et al.[4] presented a steady state analysis of simple multiple wick solar still(Fig. 1.3). Using Dunkle's relations and neglecting the heat capacity of the irradiated mass of water and the glass cover, the energy balance for the glass cover and the water sheet were expressed as

$$\tau_1 \times H_s + q_{rw} + q_{cw} + q_{ew} - q_a = 0 \quad \dots(15)$$

and

$$\tau_2 \times H_s - q_{rw} - q_{cw} - q_{ew} - h_b \times (T_b - T_a) \quad \dots(16)$$

where the terms q_{cw} , q_{ew} , q_{rw} and q_a the same as already explained in equations (4), (5), (6) and (7), respectively and

$$1/h_b = L/K + 1/h_1$$

The amount of water distilled per unit time per unit area is obtained by using Dunkle's relations.

$$m_e = q_{ew} / \lambda = \{16.273 \times 10^{-3} \times [q_{cw} (P_w - P_g)]\} / \lambda (T_w - T_g) \dots(17)$$

where the temperature of water T_w and that of the glass cover T_g were evaluated by the simultaneous solutions of the equations (15)

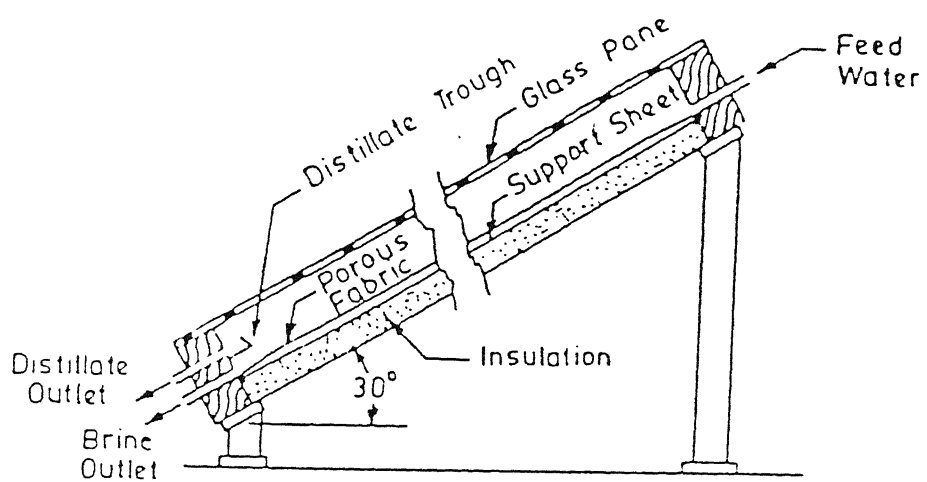


Fig.1.3 Simple multiple wick solar still.

and (16) by numerical methods.

1.5.3 DOUBLE BASIN SOLAR STILL

Tewari et al.[14] have analyzed the performance of a double basin solar still, using the periodic theory developed earlier. The major heat flux components are shown in Fig. 1.4. The heat balance equations are

$$M_{gu} \, dT_{gu} / dt = \tau_1 H_s + q_u - q_a$$

$$M_{wu} \, dT_{wu} / dt = \tau_2 H_s + h_5 (T_{gL} - T_{wu}) - q_u$$

$$M_{gL} \, dT_{gL} / dt = \tau_3 H_s + q_L - h_5 (T_{gL} - T_{wu})$$

$$M_{wL} \, dT_{wL} / dt = \tau_4 H_s + h_3 (\vartheta|_{x=0} - T_{wL}) - q_L$$

$$\tau_5 H_s = h_3 (\vartheta|_{x=0} - T_{wL}) - K_1 (\partial\vartheta/\partial x)|_{x=0}$$

where

q_u = Total heat loss from water surface in the upper basin to the upper glass surface

$$= q_{rwu} + q_{cwu} + q_{ewu}$$

q_L = Total heat loss from water surface in the lower basin to the lower glass surface

$$= q_{rwL} + q_{cwL} + q_{ewL}$$

u and L refer to upper and lower glass covers respectively and

q_{cwu} , q_{rwu} , q_{ewu} and q_{cwL} , q_{rwL} , q_{ewL} are the same as q_{cw} , q_{rw} , q_{ew} explained earlier provided T_w and T_g are replaced by T_{wu} and T_{gu} and T_{wL} and T_{gL} respectively.

Energy balance at the surface of insulation in contact with air is given by

$$- K_1 (\partial\vartheta/\partial x)|_{x=L} = h_4 (\vartheta|_{x=L} - T_a)$$

The solar insolation and ambient air temperature can be considered periodic and are given by equations (13) and (14) respectively.

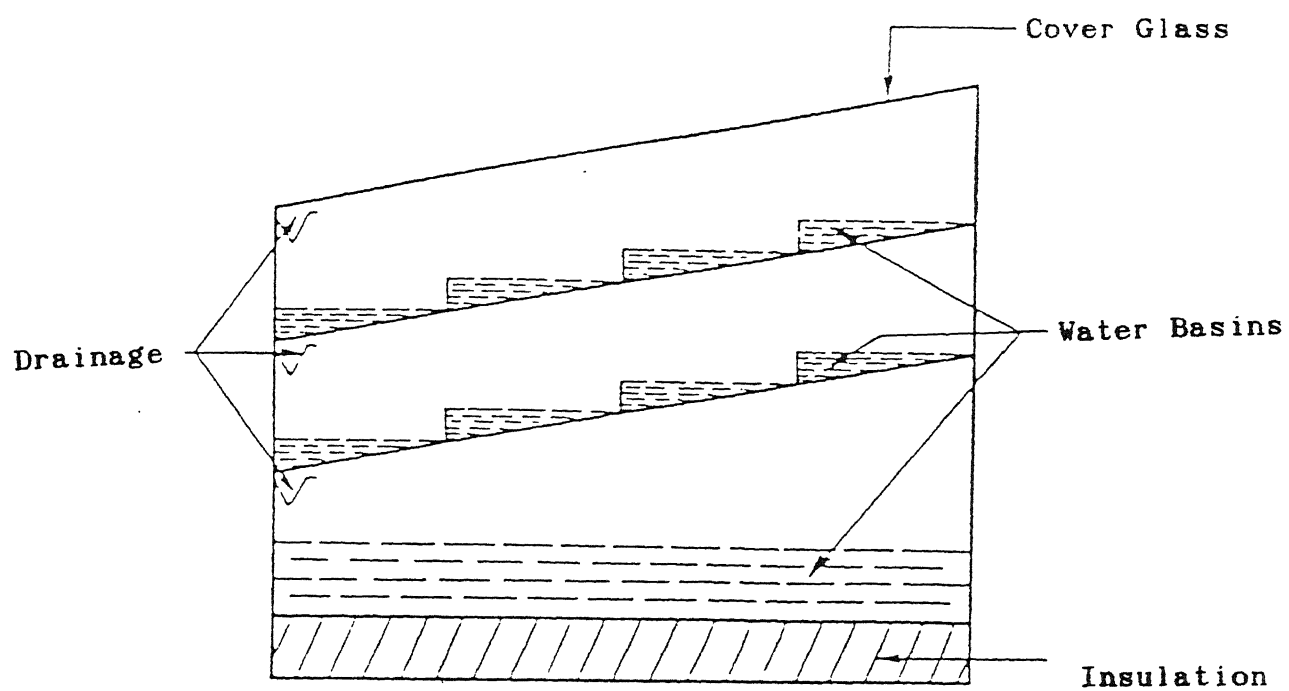


Fig.1.4 Double basin solar still

The following periodic solutions were assumed.

$$\vartheta(x,t) = A x + B + \operatorname{Re} \sum_n \{C_n \exp(-\beta_n x) + D_n \exp(\beta_n x)\} \exp(in\omega t)$$

$$T_{gu} = g_0 + \operatorname{Re} \sum_n g_n \exp(in\omega t)$$

$$T_{gL} = G_0 + \operatorname{Re} \sum_n G_n \exp(in\omega t)$$

$$T_{wu} = h_0 + \operatorname{Re} \sum_n h_n \exp(in\omega t)$$

$$T_{wL} = H_0 + \operatorname{Re} \sum_n H_n \exp(in\omega t)$$

where the constants A , B , C_n , D_n , g_0 , g_n , h_0 , h_n , G_0 , G_n , H_0 and H_n were determined from the above equations and the exact solutions obtained.

1.6 PRESENT WORK

In the works reported so far, it has been assumed that the air is saturated at all points inside the still. Besides, the design of the stills have almost been identical in the sense that all of them have been basin type stills in which a large volume of water is kept on the top of the glass plates resulting in large attenuation of solar insolation passing through the thickness of water layer and reaching the absorber plates

The present analysis of heat and mass transfer phenomena in a double-effect solar still discards a very important assumption, that the air is saturated at all points inside the still, used in previous works in this field. An improved equation for transmission of solar radiation as suggested by P.T.Tsiligris [20] has also been used. Besides, the design of the still being investigated is such that it exposes a larger water surface to the solar radiation as compared to the solar stills of same dimensions analyzed in previous works. There is a continuous flow of water in

the lower stage of the still over the absorber plate which is in contrast to the solar stills analyzed in earlier investigations.

In the present work, a computer model of a double-effect solar still has been developed. The input to the program are the hourly and monthly solar radiation and ambient temperature data for New Delhi chosen as a representative North Indian location. Also information about the dimensions of the still, operating conditions and thermophysical properties of water and air are provided.

CHAPTER - 2

MATHEMATICAL MODEL

The double-effect solar still, considered in the present work, consists of three distinct plates: the top glass cover, the intermediate glass plate and the absorber plate. The thermal performance of such a still depends on the heat capacity of these three plates.

Figure 2.1 shows a schematic diagram of the aforesaid solar still to be analyzed. The still consists of one glass cover at the top and one absorbing plate at the bottom, as well as one glass plate in the middle; all of these plates are parallel. In order to collect more insolation, the equipment is tilted from the horizontal, with the cover inclined towards the sun. Accordingly, several weirs are installed in parallel on the upper surface of the glass plate to hold the saline water, while a blackened wet jute cloth is placed on the upper surface of the absorbing plate to form the liquid surface. Except for the glass cover, all parts of the enclosure are carefully insulated with a thick layer of asbestos to make the heat loss as low as possible. During operation, the top glass cover and intermediate glass plate transmit solar radiation and the absorbing plate is then heated directly by solar radiation. The saline water feeds are introduced on the upper surfaces of both the absorbing and intermediate glass plates, where some water evaporates, while the remainder is collected at the bottom and discarded as concentrated brine. The

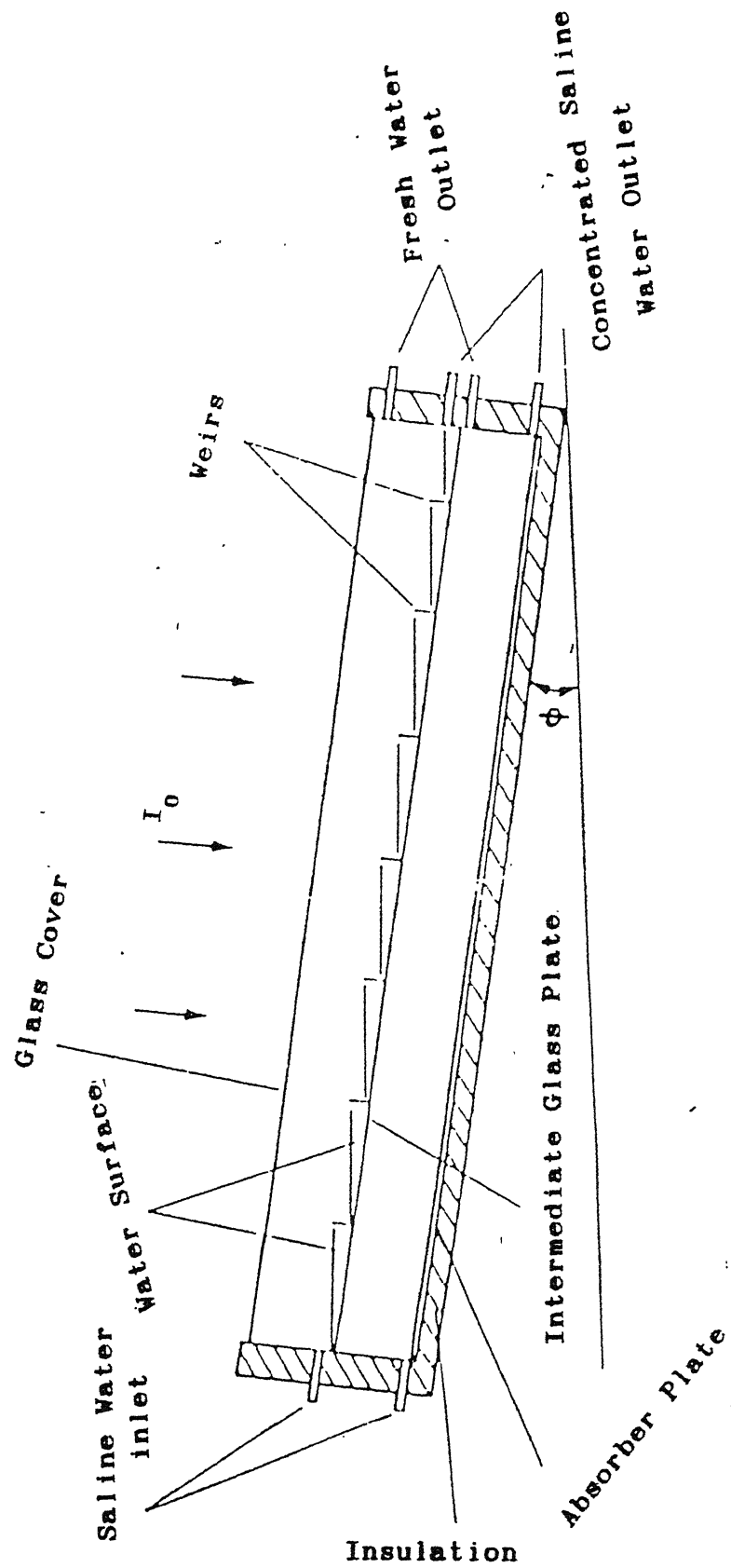


Fig.2.1 Schematic diagram of Double-Effect solar still

vapor produced from the saline water rises from the absorbing plate and is condensed on the lower side of the intermediate glass plate. The heat of condensation given up by the condensing vapor on the lower side of the glass plate is conducted through this plate and furnishes heat to evaporate an equivalent amount of water from the saline water sliding down the upper side of the plate. Finally, the heat of condensation given up by the condensing vapor on the lower side of the glass cover is transmitted through this cover to the ambient. The condensates produced from the first and second effects are collected as fresh water in a trough from the enclosure.

2.1 DEVELOPMENT OF THE MODEL

The still is considered to be one dimensional with respect to the heat transfer, with the temperature drop through the cover and the plate thickness being neglected. Besides, the air at the water surface may be considered to be saturated while that at the condensing surface may be unsaturated or supersaturated. This assumption made in the present study is a significant departure from the earlier theoretical analyses which have assumed that water is saturated at all points inside the still. The model considers the transmission of the incident solar radiation through the surface, its attenuation as it passes through the subsequent water layers and the final absorption in the absorber plate. The blackened jute cloth is assumed to be perfectly absorbing and the radiation incident on it is completely absorbed there. It is further assumed that there are no losses from the bottom and sides of the still, these being perfectly insulated from the surroundings. The temperature of the absorber plate being higher

than that of other plates, it loses heat to the intermediate glass plate which loses heat to the glass cover and the glass cover losing heat to the surroundings by convection and radiation.

The above mentioned processes are discussed in detail in the ensuing sections and presented in a mathematical form, using basic principles of heat transfer.

2.2 ATTENUATION OF SOLAR RADIATION IN A WATER LAYER

The performance of a solar still largely depends on the amount of the radiation which reaches the absorber plate at the bottom of the still.

The most widely used mathematical expression on transmission of solar radiation through a water layer in literature is the Rabl and Nielson [11] four term exponential expression given by

$$f(z) = \mu_i \times I_0 \sum_{i=1}^4 \exp(-n_i z) \dots(1)'$$

where μ_i and n_i are empirical coefficients and have different values for different wavelength bands.

For water thicknesses in the range from 1 cm to 10.0 m a relation for the fraction of incident solar energy $f(z)$ transmitted through a thickness of z cm was obtained by BRYANT and COLBECK[10], as

$$f(z) = a' - b' \ln(z) \dots(2)$$

where $a' = 0.73$ and $b' = 0.08$ ($a' = 0.36$ if z is in meters). This representation is simpler for use than that of RABL and NEILSON. However, for a water thickness < 1.0 cm, Eq (1) is not accurate, especially for the region very close to water surface. For this reason, a modified expression [19] for $f(z)$ in this particular

region is introduced as follows:

$$f(z) = a - b \ln(z+c) \quad \dots(3)$$

Here the constants a , b and c of Table 2.2 have been determined from the experimental data given in Table 2.1. The comparison of Eq(3) with Eq(2), as well as with RABL and NEILSON's expression, are presented in Figure 2.2. It is seen from this figure that Eq(2) is the most accurate for the range of water thickness from 0 to 1.0 cm.

2.3 ABSORPTIVITY AND TRANSMITTANCE OF A WATER LAYER ON A GLASS PLATE

If the reflection of solar insolation at the surface of a water layer on the upper surface of a glass plate is neglected, then

$$\tau_w + \alpha_w = 1 \quad \dots(4)$$

As shown in Figures 2.1 and 2.3, we consider the optimal design case in which the height of weirs, as well as the distances between the weirs, are so installed that the depth of water layer at one end is exactly zero. Thus, the depth of water layer is related to the y -axis by

$$z = p \times (1 - y/L) \quad \dots(5)$$

Since the solar energy flux transmitted through the glass cover is $(\tau_g \times I_0)$, that transmitted through the water layer on the glass plate may be calculated from

$$(\tau_g \times I_0) \times \tau_w = (1/W \times L) [(\tau_g \times I_0) \int_0^L f(z) \times W dy]$$

$$\text{Hence, } \tau_w = (1/W \times L) \left[\int_0^L f(z) \times W dy \right] \quad \dots(6)$$

From Eq (5) we have

$$dz = -(p/L) \times dy \quad \dots(7)$$

λ (μm)	z							
	0mm	0.01mm	0.1mm	1mm	1cm	10cm	1m	10m
0.2-0.6	23.7	23.7	23.7	23.7	23.7	23.6	22.9	17.2
0.6-0.9	36.0	36.0	36.0	35.9	35.3	30.5	12.9	0.9
0.9-1.2	17.9	17.9	17.8	17.2	12.3	0.8	-	-
1.2-3.0	8.7	8.6	8.2	6.3	1.7	-	-	-
1.5-1.8	8.0	7.8	6.4	2.7	-	-	-	-
1.8-2.1	2.5	2.3	1.1	-	-	-	-	-
2.1-2.4	2.5	2.4	1.9	0.1	-	-	-	-
2.4-2.7	0.7	0.6	0.2	-	-	-	-	-
2.7-3.0	-	-	-	-	-	-	-	-
Total	100.0	99.3	95.3	85.9	73.0	54.9	35.8	18.1

Table 2.1 The fraction of incident energy remaining after passing through a thickness of z , in various range of wavelength,

z , cm	a	b	c , cm
$0 \sim 0.1$	0.749	0.0492	6.0×10^{-3}
$0 \sim 1.0$	0.732	0.0560	8.4×10^{-3}
$0 \sim 10.0$	0.716	0.0688	0.0173
$0 \sim 1.0 \times 10^2$	0.716	0.0754	0.0256
$0 \sim 10.0 \times 10^2$	0.716	0.0768	0.0282

Table 2.2 Values of a , b and c for various water thicknesses

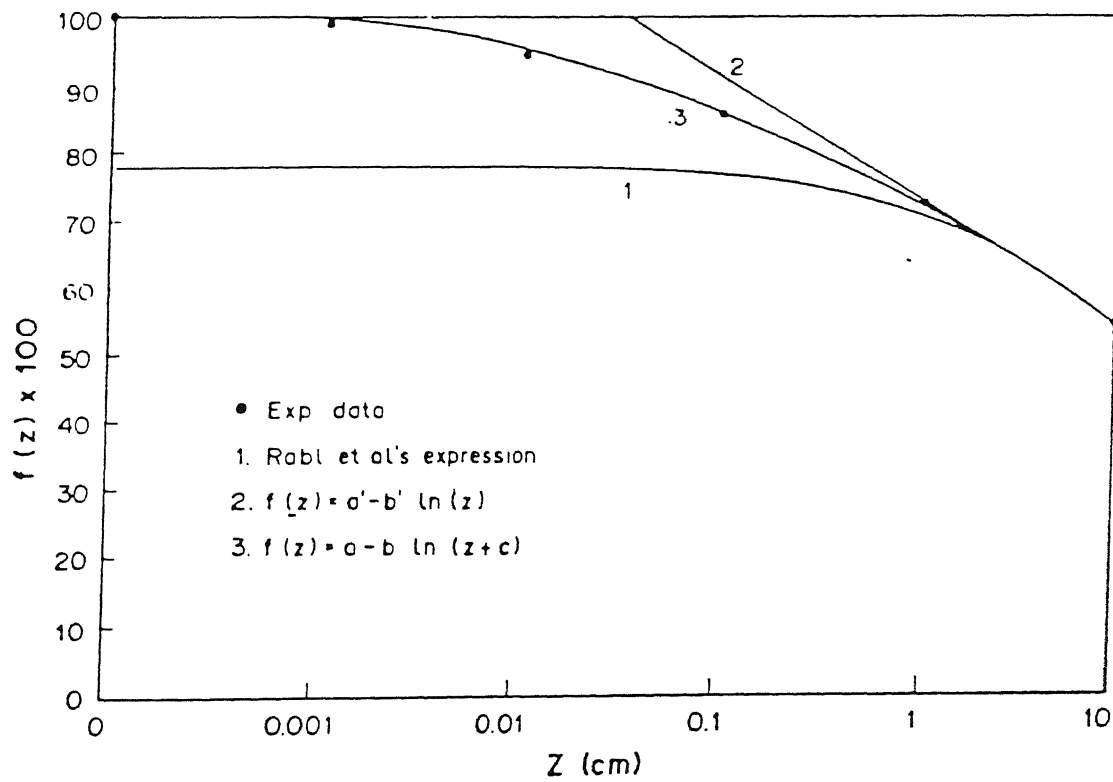


Fig.2.2 Fraction of incident energy remaining after passing through a thickness z

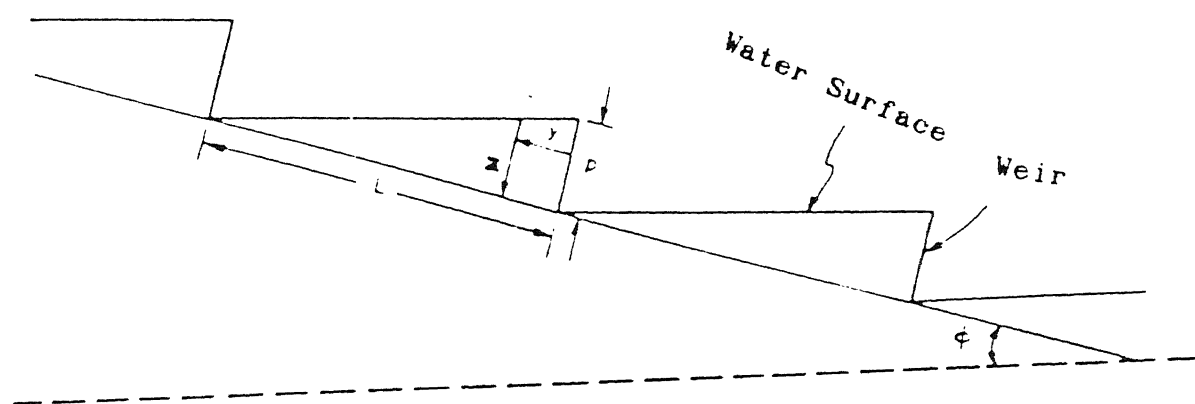


Fig.2.3 Water layers on the glass plate

Using the expression for $f(z)$ from Eq(3) and using Eq(5), the expression in Eq(6) reduces to

$$\tau_w = (1/W \times L) \int_0^p \{a - b \ln(z+c)\} \times (L/p) dz \quad \dots(8)$$

Performing the integration in Eq(8), we get

$$\begin{aligned} \tau_w &= (1/p) \times \{a \times p - b \times p \ln(p+c) + b \int_0^p [z/(z+c)] dz\} \\ &= (1/p) \times \{a \times p - b \times p \ln(p+c) + b \times p - b \times c \ln(p+c) + b \times c \ln(c)\} \\ &= \{a - b \times [(p+c)/p] \times \ln(p+c) - (c/p) \times \ln(c) - 1\} \quad \dots(9) \end{aligned}$$

The solar energy flux absorbed by the water layer is obtained by using Eq(4) and the fact that

$$f(0) = 1 = a - b \times \ln(c)$$

Hence,

$$\begin{aligned} \alpha_w &= (1 - \tau_w) \\ &= b \{[(p+c)/p] [\ln(p+c)/c] - 1\} \quad \dots(10) \end{aligned}$$

2.4 GOVERNING EQUATIONS

2.4.1 ENERGY BALANCE FOR THE TOP GLASS COVER

The energy exchange of the glass cover with the ambient and the transparent plate is shown in Fig. 2.4. The glass cover is assumed to be at a uniform temperature T_c . The glass cover receives I_0 energy from the sun part of which is absorbed by it and some part of it is reflected while most of it is transmitted through it.

$$\text{Incident radiation energy absorbed} = \alpha_g \times I_0$$

$$\text{Incident radiation energy transmitted through glass cover} = \tau_g \times I_0$$

$$\text{Evaporation heat gain from intermediate glass plate} = Q_{e2}$$

$$\text{Convective heat gain from intermediate glass plate} = Q_{c2}$$

$$\text{Radiative heat gain from intermediate glass plate} = Q_{r2}$$

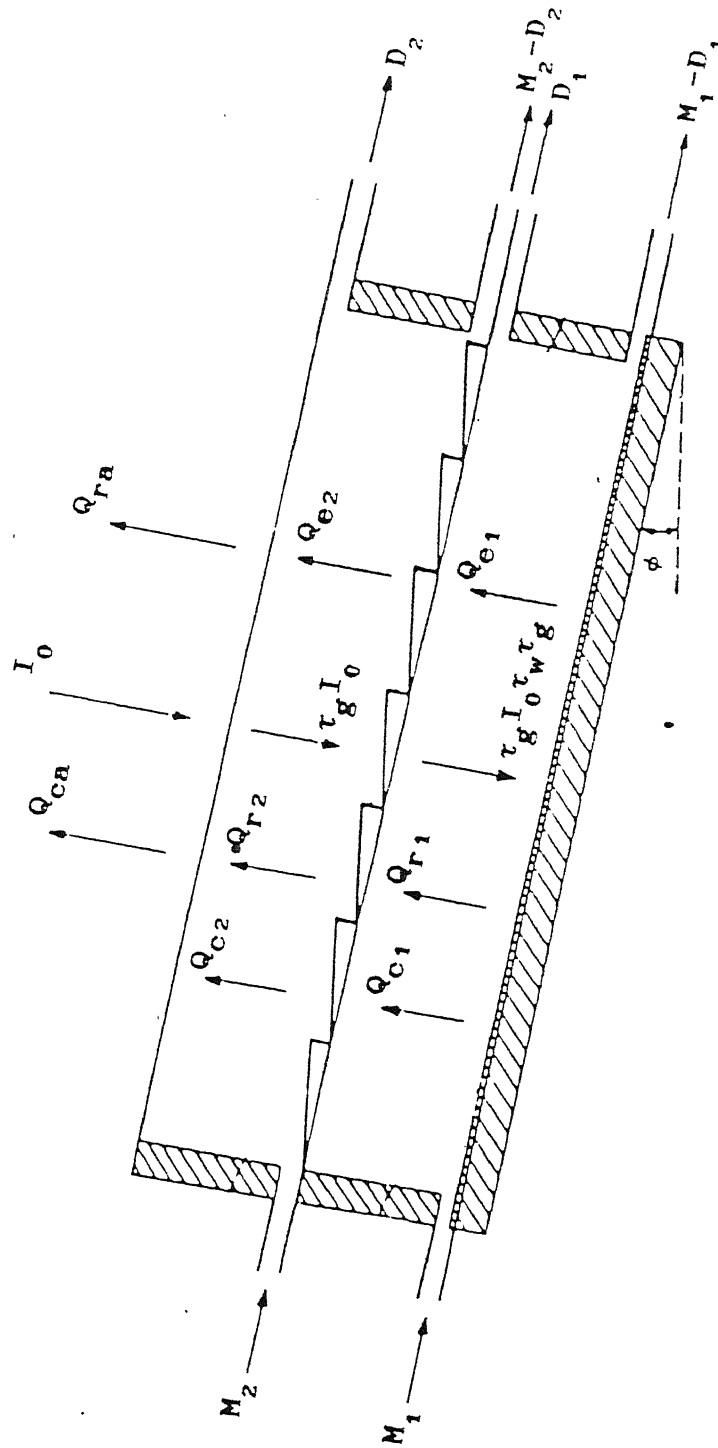


Fig.2.4 Energy Fluxes in Double-Effect solar still

Convective energy loss from cover to ambient $= Q_{ca} = h_a (T_c - T_a)$

where h_a , the wind convective heat transfer coefficient [7], is given by

$$h_a = 5.7 + 3.8 \times V, \quad W/m^2-K$$

where V is wind velocity in m/s

Energy lost by radiation to the surroundings $= Q_{ra} = \epsilon_g \sigma (T_c^4 - T_a^4)$

Using the above expressions, we can write the total inward flux of the glass cover as

$$\alpha_g I_0 + Q_{e2} + Q_{c2} + Q_{r2}$$

and the total outward flux of the glass cover as

$$Q_{ca} + Q_{ra}$$

considering steady state performance of the still, we can write

$$\alpha_g \times I_0 + Q_{e2} + Q_{c2} + Q_{r2} = Q_{ca} + Q_{ra} \quad \dots (11)$$

where

$$Q_{e2} = \epsilon_{\lambda_2} \times D_2$$

$$Q_{c2} = (h_{wgc} \times A_w + h_{weg} \times A_{we}) \times (T_2 - T_c) / A_b$$

$$Q_{r2} = 0.9 \times \sigma \times (T_2^4 - T_c^4)$$

$$A_w = A_b / \sin \phi$$

$$A_{we} = A_b \times \tan \phi$$

2.4.2 ENERGY BALANCE FOR THE INTERMEDIATE GLASS PLATE

On the intermediate glass plate, as the depth of water mass on the plate increases, the fraction of energy incident on the plate decreases. The energy flux terms in the intermediate glass plate are as shown in Fig. 2.4.

The intermediate glass plate being at a higher temperature than the glass cover loses heat to the cover while it receives energy from the absorbing plate. It also absorbs a portion of the incoming solar radiation. The above mentioned energy flux terms

for the plate can be expressed mathematically as:

Solar Energy absorbed by the water mass on the plate = $\tau_g \times I_0 \times \alpha_w$

Solar energy absorbed by intermediate glass plate = $(\tau_g I_0) \tau_w \alpha_g$

Evaporative heat flux from the absorbing plate = Q_{e1}

Convective heat flux from the absorbing plate = Q_{c1}

Radiative energy flux from the absorbing plate = Q_{r1}

Also there is an energy input to the plate in the form of inlet water at temperature T_1 while there is an energy loss due to the outflow of concentrated brine at temperature T_2 . Besides this, the water vapor that condenses at temperature T_2 leaves the plate at temperature T_2 .

Hence the energy balance equation of the intermediate glass plate is given by

$$\begin{aligned} & (\tau_g \times I_0) \times \alpha_w + (\tau_g \times I_0) \times \tau_w \times \alpha_g + M_2 \times C_{p_w} \times (T_1 - T_c) + Q_{e1} + Q_{c1} + Q_{r1} \\ & = (M_2 - D_2) \times C_{p_w} \times (T_2 - T_c) + D_1 \times C_{p_w} \times (T_2 - T_c) + Q_{e2} + Q_{c2} + Q_{r2} \\ & \dots\dots\dots(12) \end{aligned}$$

where

$$Q_{e1} = \lambda_1 \times D_1$$

$$Q_{c1} = h_1 \times (T_1 - T_2)$$

$$Q_{r1} = \epsilon_w \times \sigma \times (T_1^4 - T_2^4)$$

HOLLANDS [7] obtained an empirical expression for the heat transfer coefficients in free convection of an inclined layer of high aspect ratio, heated from below, as follows:

$$\begin{aligned} Nu_{wgc} &= h_{wgc} H_2 / K_a \\ &= 1 + 1.44 \times [1 - (1708 / RA_{wgc} \cos \phi)]^+ \times [1 - 1708 \times \sin(1.8 \phi)^{1.6} / RA_{wgc} \cos \phi] \\ &+ [(RA_{wgc} \cos \phi / 5830)^{1/3} - 1]^+ \dots\dots\dots(13) \end{aligned}$$

$$RA_{wgc} = (g H_2^3 \beta / \nu_a \alpha) [(T_2 - T_c) + \{(P_{s,2} - F_c \times P_{s,c}) / (2.65 \times P_t - P_{s,2})\} T_2]$$

where $X^+ = (|X| + X) / 2$

$$\text{and } \alpha = K_a / \rho_a C_{p_a}$$

$$\text{and } F_c = 0.606[(T_2 - T_c)/H_2]^{0.119}$$

F_c is the modified factor for glass cover since the air at the water surface may be considered to be saturated while that at the condensing surface may be saturated or supersaturated [19].

For free convection from a vertical plate, the following correlations, given by CHURCHILL and CHU[22], have been used.

$$Nu_{weg} = h_{weg} p / K_a = 0.68 + 0.67 \times RA_{weg}^{1/4} / [1 + (0.492/Pr)^{9/16}]^{4/9} \quad \dots (14)$$

$$Pr = C_{p_a} \times \mu_a / K_a$$

$$RA_{weg} = g \times \cos \phi \times p^3 \times \beta \times (T_2 - T_c) / \nu_a \alpha$$

Similarly,

$$Nu_1 = h_1 H_1 / K_a = Nu_{wgc} | RA_1 \longrightarrow RA_{wgc} \quad \dots (15)$$

$$RA_1 = (g H_1^3 \beta / \nu_a \alpha) [(T_1 - T_2) + (P_{s,1} - F_2 \times P_{s,2}) \times T_1 / (2.65 \times P_t - P_{s,1})]$$

where modified factor F_2 is given by [19]

$$F_2 = 0.512[(T_1 - T_2)/H_1]^{0.273}$$

2.4.3 ENERGY BALANCE FOR THE ABSORBING PLATE

The energy flux terms for the absorber plate are shown in Fig. 2.4. The absorbing plate receives energy from the solar radiation transmitted through the glass cover, the water mass and the intermediate glass plate. The energy balance equation for the absorbing plate can be written as follows:

$$(\tau_g \times I_o) \times \tau_w \times \tau_g + M_1 \times C_{p_w} \times (T_i - T_c) = Q_{e1} + Q_{c1} + Q_{r1} + (M_1 - D_1) \times C_{p_w} \times (T_1 - T_c) \quad \dots (16)$$

In case of the absorbing plate, it has been assumed that, except for the glass cover, all parts of the enclosure are carefully insulated so that the heat loss from the outside surface of the absorbing plate to the ambient may be neglected. In addition, the absorptivity of water film on the absorbing plate with blackened wet jute cloths, is assumed to be unity.

2.4.4 BALANCING OF EVAPORATION RATES

Considering the second effect, the mass of air transferred per unit area per unit time by free convection is given by

$$\dot{m}_{a2} = Q_{c2} / C_{p_a} \times (T_2 - T_c)$$

Therefore,

$$D_2 C_{p_a} (T_2 - T_c) M_{a2} = (h_{wgc} \times A_w + h_{weg} \times A_{we}) \times (T_2 - T_c) / A_b \quad \dots (17)$$

where

$$M_{a2} = 1 / (W_{s,2} - W_c) \\ = 1 / \{ (M_w / M_a) [P_{s,2} / (P_t - P_{s,2}) - F_c P_{s,c} / (P_t - F_c P_{s,c})] \} \quad \dots (18)$$

Combining eq.(14) and (15), we get

$$D_2 = (M_w / M_a C_{p_a}) [(h_{wgc} A_w + h_{weg} A_{we}) / A_b] [P_{s,2} / (P_t - P_{s,2}) - F_c P_{s,c} / (P_t - F_c P_{s,c})] \\ = 2.59 [(h_{wgc} A_w + h_{weg} A_{we}) / A_b] [P_{s,2} / (P_t - P_{s,2}) - F_c P_{s,c} / (P_t - F_c P_{s,c})] \quad \dots (19)$$

Similarly, for first effect proceeding again as above for D_2 , we get

$$D_1 = 2.59 h_1 [P_{s,1} / (P_t - P_{s,1}) - F_2 P_{s,2} / (P_t - F_2 P_{s,2})] \quad \dots (20)$$

Thus, there exist five unknown variables T_1 , T_2 , T_c , D_1 and D_2 which have been determined by solving eqs.(11),(12),(14),(19),(20) numerically, as described in the next section.

2.5 NUMERICAL SOLUTION

The set of five equations are numerically solved on the computer, HP 9000/850 system. The following paragraphs are devoted to the explanation of the development of the program [Appendix A].

The equations involved are non-linear functions of five different variables and the use of a computer facilitates the determination of the variables. The program uses the services of NAG LIBRARY for the solution of these equations. It uses the SUBROUTINE CO5NBF(from NAG LIBRARY), the purpose of which is to find a zero of a system of N non-linear functions in N variables by a modification of POWELL's HYBRID method. It uses a Jacobian,calculated by forward difference approximation. It requires an external subroutine ,to be supplied by the user, which calculates the value of the functions of the N variables [Appendix A].

Since, hourly and monthly data of temperature and solar insolation of NEW DELHI are available from the literature[2], these are fed as the input data to the computer program. The design (width and length of still, chamber height of the two stages, weir height), climatic (solar insolation, ambient temperature and ambient velocity) and operational (total pressure, mass flow rate in the lower basin) parameters are given as inputs to the program.

The initial part of the program is devoted to the calculation of various heat transfer coefficients using the initial input data and the initial approximation. Also, the various tilt angles of the still during different parts of the year are used to calculate the various terms occurring in the equations These heat transfer

coefficients are calculated by using the values of RAYLEIGH NUMBERS yielded by various empirical correlations mentioned earlier. These heat transfer coefficients are then used to calculate the various heat transfer terms occurring in the equations. These equations in the form of non-linear functions are then used by subroutine C05NBF to calculate a converging solution to the five equations.

CHAPTER - 3

RESULTS AND CONCLUSIONS

3.1 INPUT DATA

To compute the distillate production and the temperatures of the various plates of the double-effect still, monthly and hourly meteorological data for New Delhi were utilized. This data have been utilized in Fig. 3.1 which shows the monthly variation of global solar radiation for New Delhi. It can be seen that maximum global solar radiation is received in the month of May, where after it drops rapidly except for a small rise in the month of September.

3.2 DISCUSSION OF RESULTS

The temperatures of the cover, the intermediate glass plate and the absorber plate and the net distillate production have been calculated using the computer program as discussed earlier.

Fig. 3.2 gives the variation of temperature with the month of the year for the cover, the intermediate glass plate and the absorber plate. It is seen that the general trend for the variation of temperatures follows closely the variation of global solar radiation with the month of the year [Fig. 3.1]. Thus, the maximum temperatures are recorded in May. As expected, the absorber plate shows the highest temperature and the cover the lowest throughout the year. For example, in the month of March, temperature calculations for the cover, the intermediate plate and the absorber plate are 324 K, 333 K and 345 K, respectively.

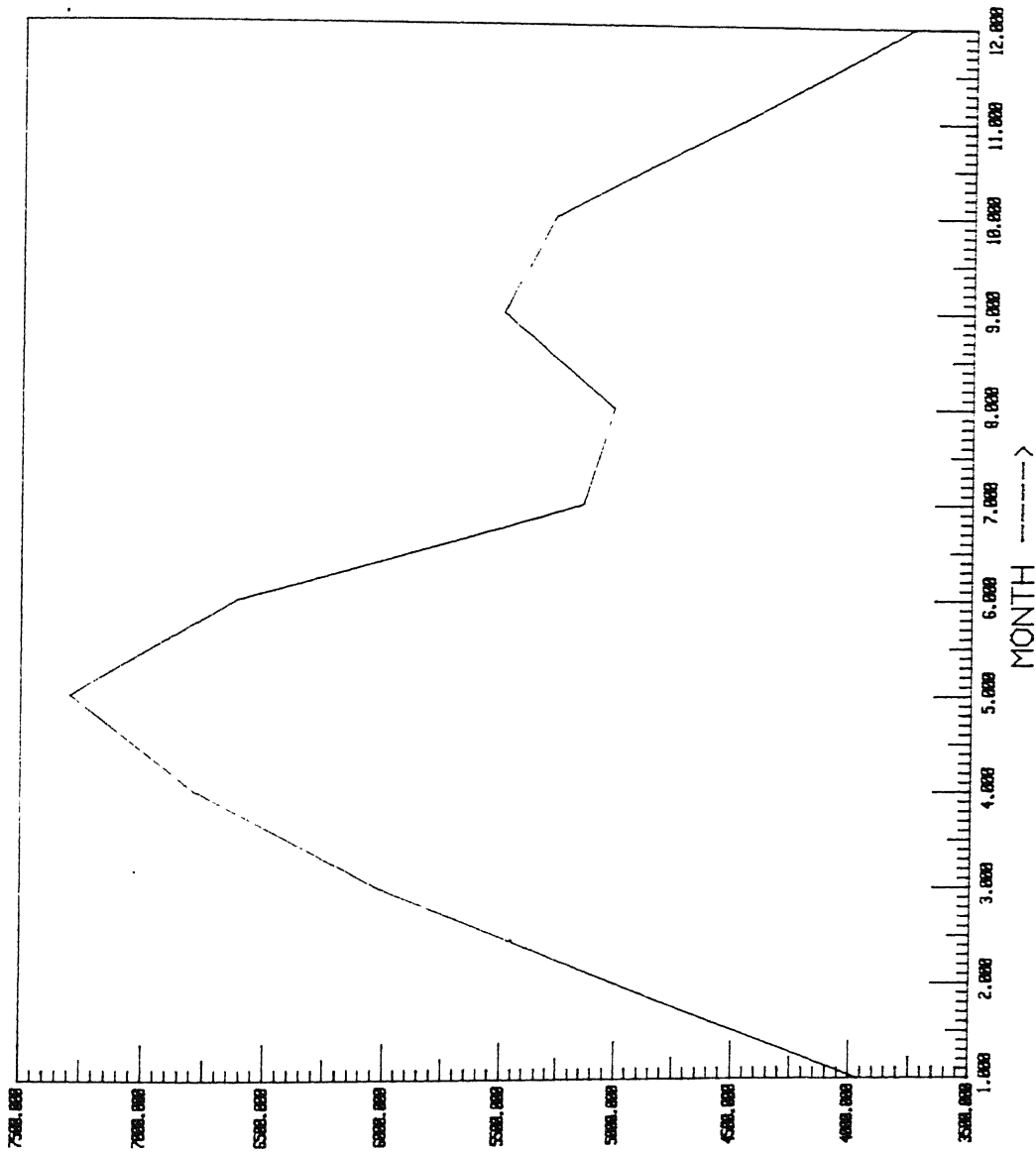


Fig.3.1 Average daily values of global solar radiation
for New Delhi

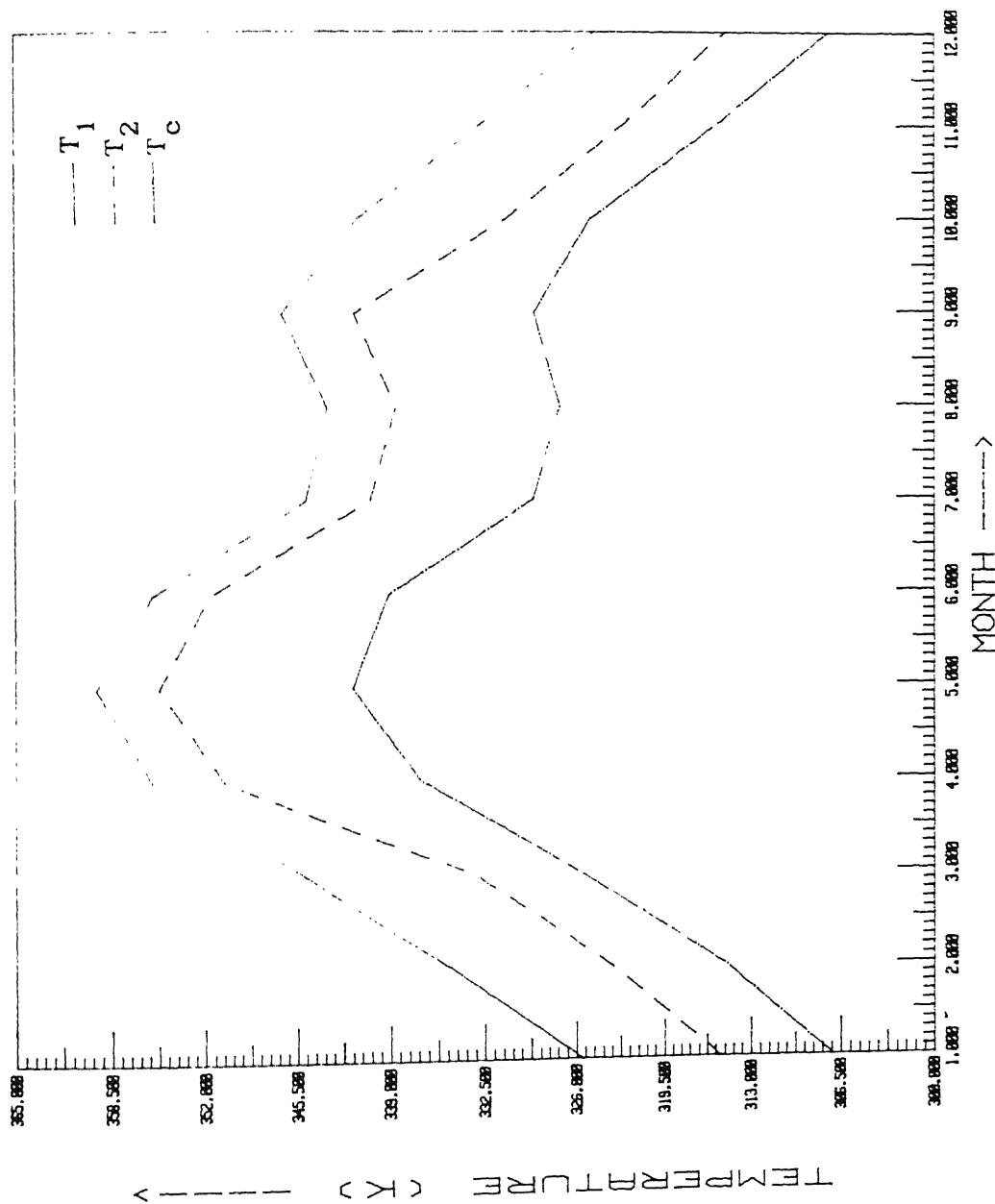


Fig.3.2 Variation of temperature of the cover, the intermediate glass plate and the absorber plate

Fig. 3.3 shows the variation of distillate outputs for the first and second effects separately with the month of the year and Fig. 3.4 depicts the total distillate output of the double-effect still in comparison with the single-effect still. It can be seen from Fig. 3.3 that the output from the second stage of the still is higher than that from the first stage. This is due to the fact that in addition to the solar radiation absorbed by the intermediate glass plate and the water mass on the plate, the vapor evaporating from the first stage and condensing on lower side of the intermediate glass plate, evaporates an equivalent amount of water from the second stage by giving up its latent heat of condensation.

The efficiency of the double effect solar still is defined as

$$\eta = \lambda \times (D_1 + D_2) / I_0$$

where D_1 and D_2 are the distillate outputs of the first and second effects.

Fig. 3.5 compares the efficiencies of the single and the double effect stills. It can be readily seen that the efficiency of the double effect still is about 35 to 40 percent higher than the single effect solar still. It is also observed that the efficiencies of both types of still are higher for higher levels of insolation. However, the efficiency varies within a narrow range of 53.5 to 64 percent for a double-effect still as against a range of about 35 to 48 percent for a single effect still. It is to be noted that, although, the range of monthly variation of solar insolation is quite large, the corresponding range of variation in efficiency of both types of solar still is small. This is due to the fact that at higher levels of

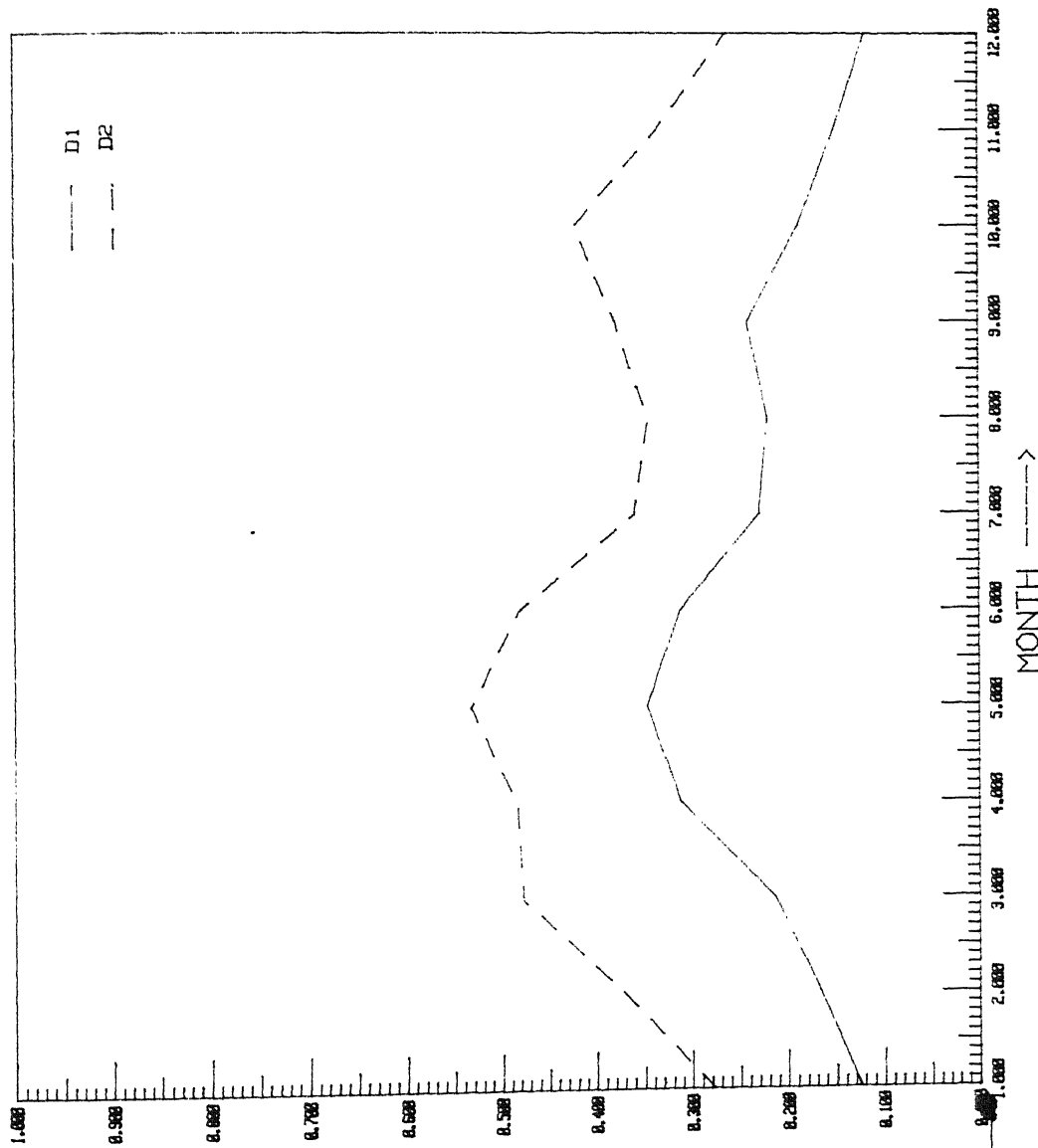


Fig.3.3 Distillate outputs from the first and second effects

DISTILLATE OUTPUT (Kg/30-5) > > > > >

DISTILLATE OUTPUT (Kg/month) > > > > >

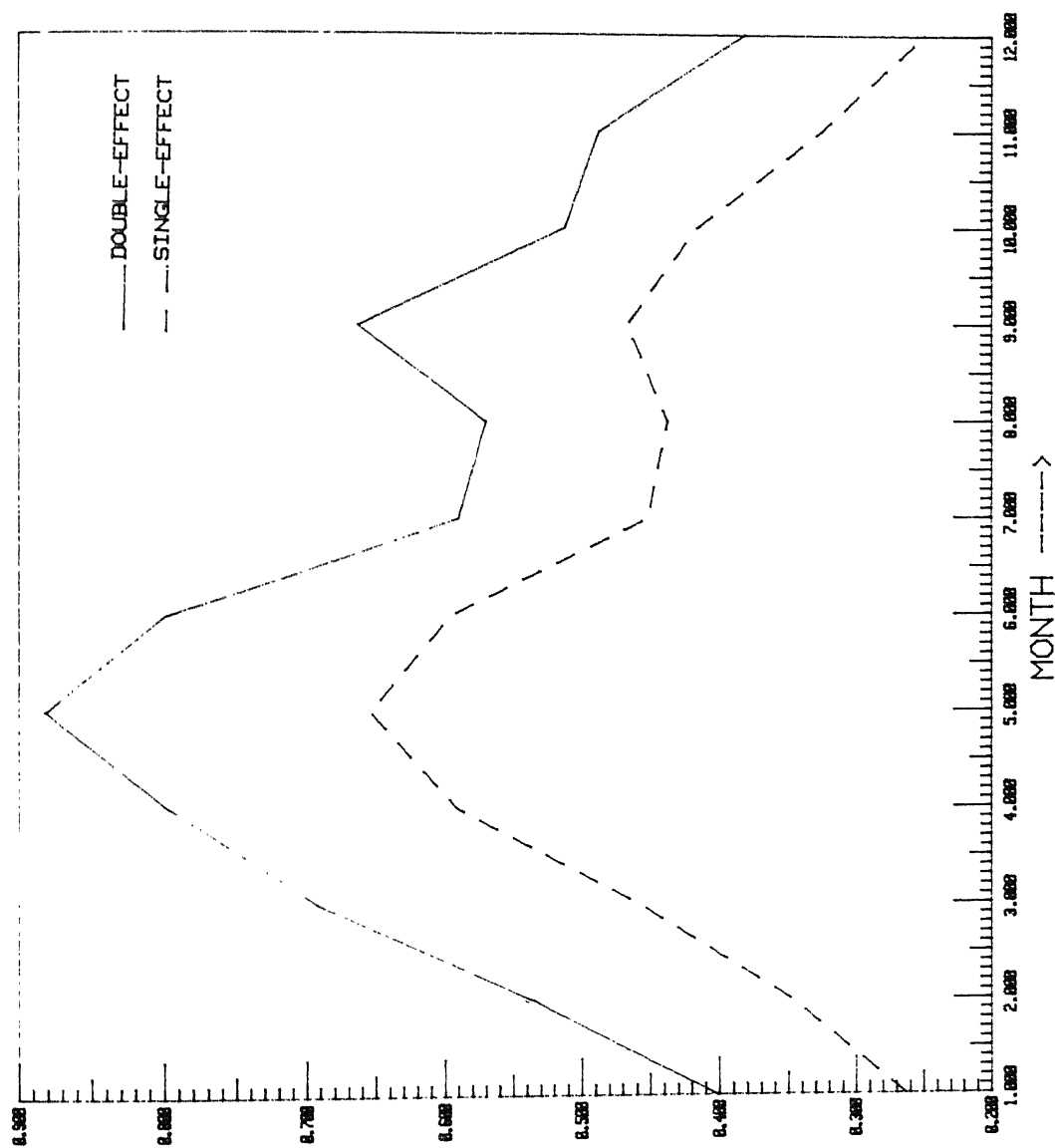


Fig.3.4'Comparison of distillate outputs of the single and double-effect stills

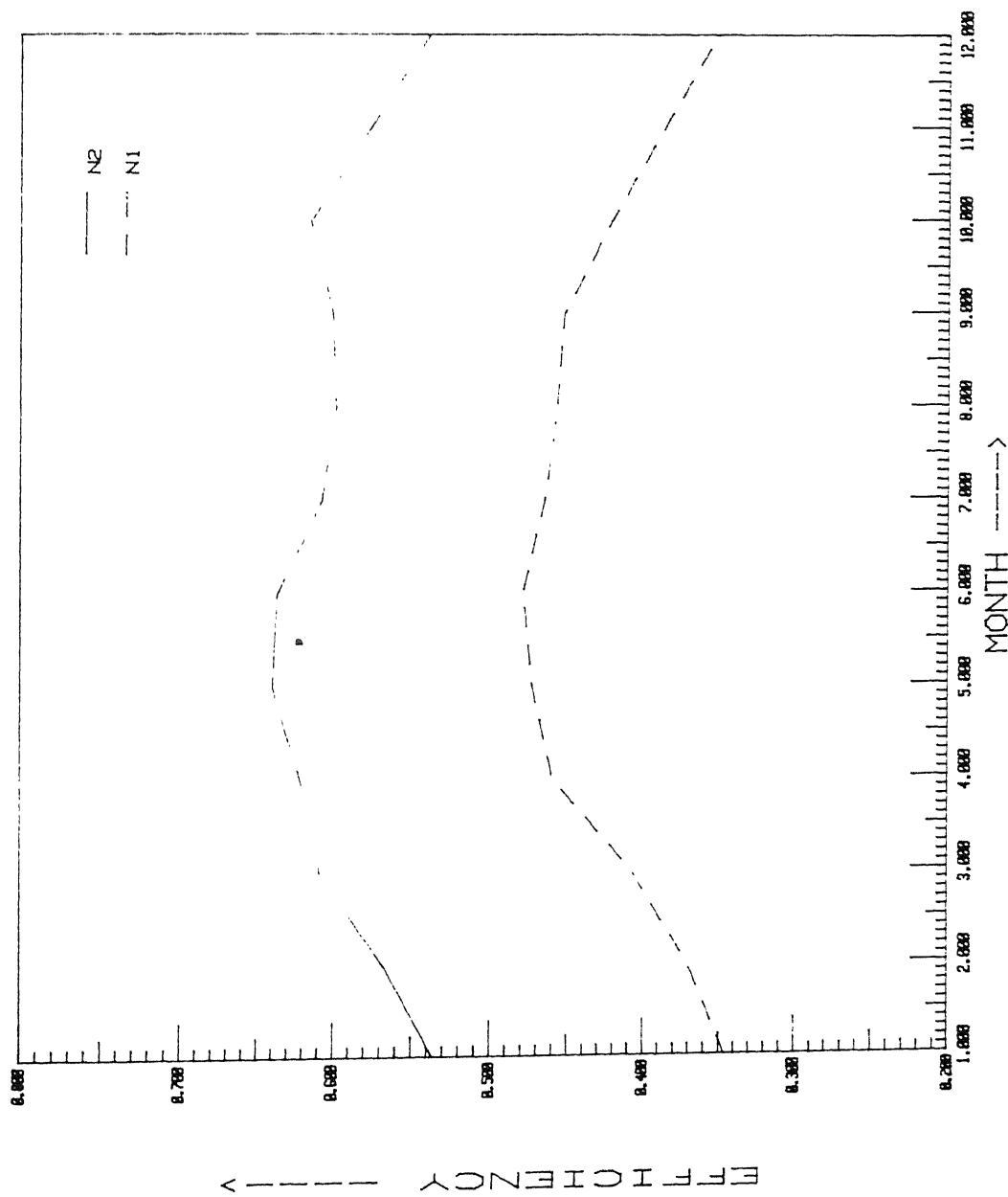


Fig.3.5 Comparison of efficiencies of single and double-effect stills

insolation, the losses are also significant.

Fig.3.6a displays the hourly variation of global solar radiation on a typical day of March for New Delhi. Fig. 3.6b gives the variation of the temperatures for the cover, the intermediate glass plate and the absorber plate with the time of the day. Fig. 3.6c shows the total distillate output for the double effect still based on hourly solar radiation data. Figs. 3.6a to 3.6c all comprise smooth curves and thus highlight the nearly continuous variation of different variables over a period of a day in March for New Delhi.

Fig. 3.7 demonstrates the variation of distillate output with ambient air velocity. For a typical day in the month of March for NEW DELHI, the ambient air velocity varies between 0 to 10 m/s[1]. It can be easily seen that as the velocity of the ambient air increases, the net distilled water production rate drops. It is maximum for the still air (i.e. velocity of 0 m/s) and gradually decreases as the velocity increases. This is apparently due to the fact that, although, the heat losses from the cover increase, due to the increased air velocity, resulting in lower cover temperatures, there is a fall in the temperature of the intermediate glass plate and the absorber plate with the net result that the effective difference between the plate temperatures decreases, thereby causing a drop in overall distillate output. This result is in agreement with the theory propounded by LOF et al., that there should be a drop in the distillate production rate with an increase in ambient air velocity. The same type of results are reported by YEH [18] in the analysis of a single effect still.

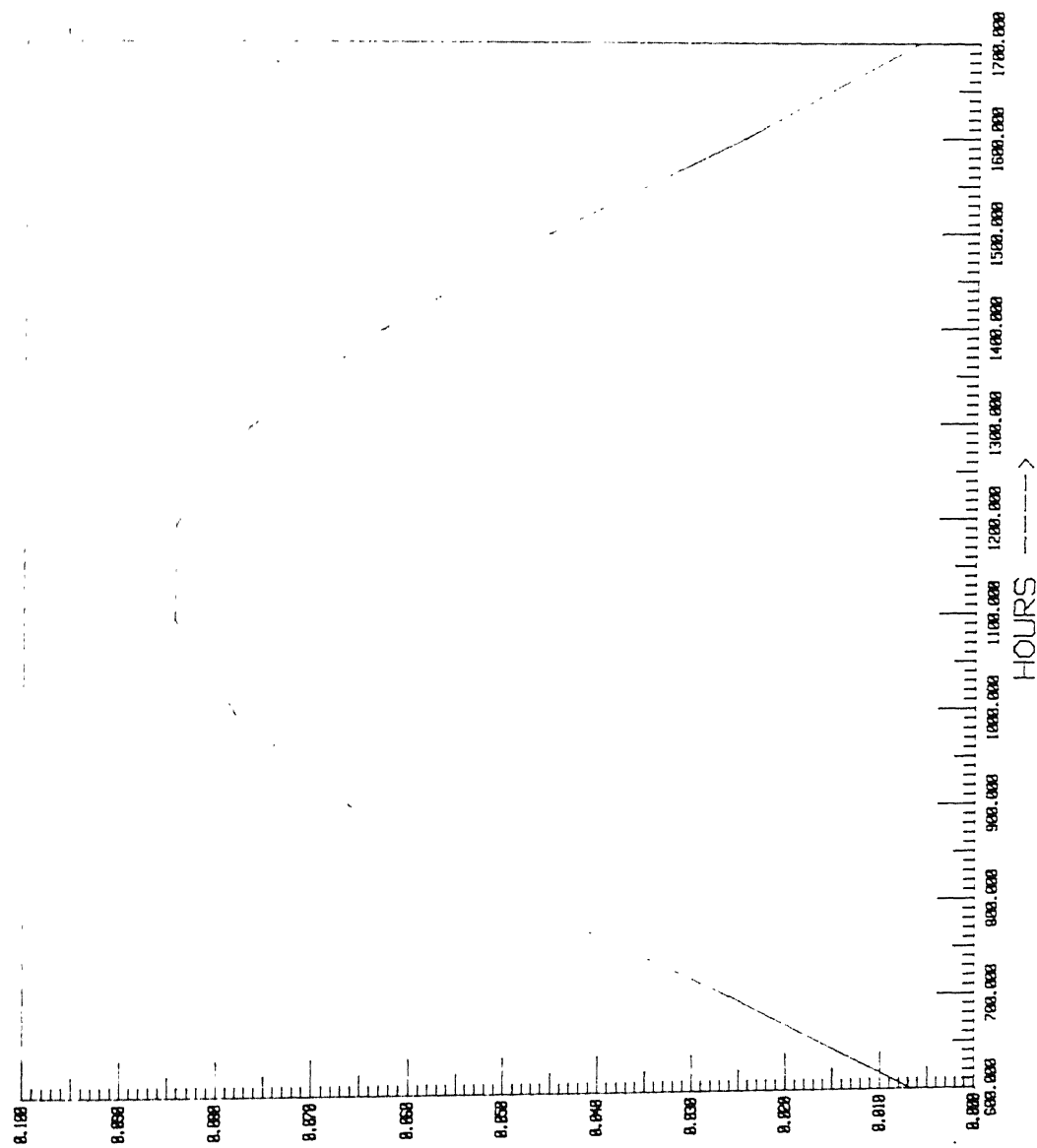


Fig.3.6a Hourly variation of global solar radiation

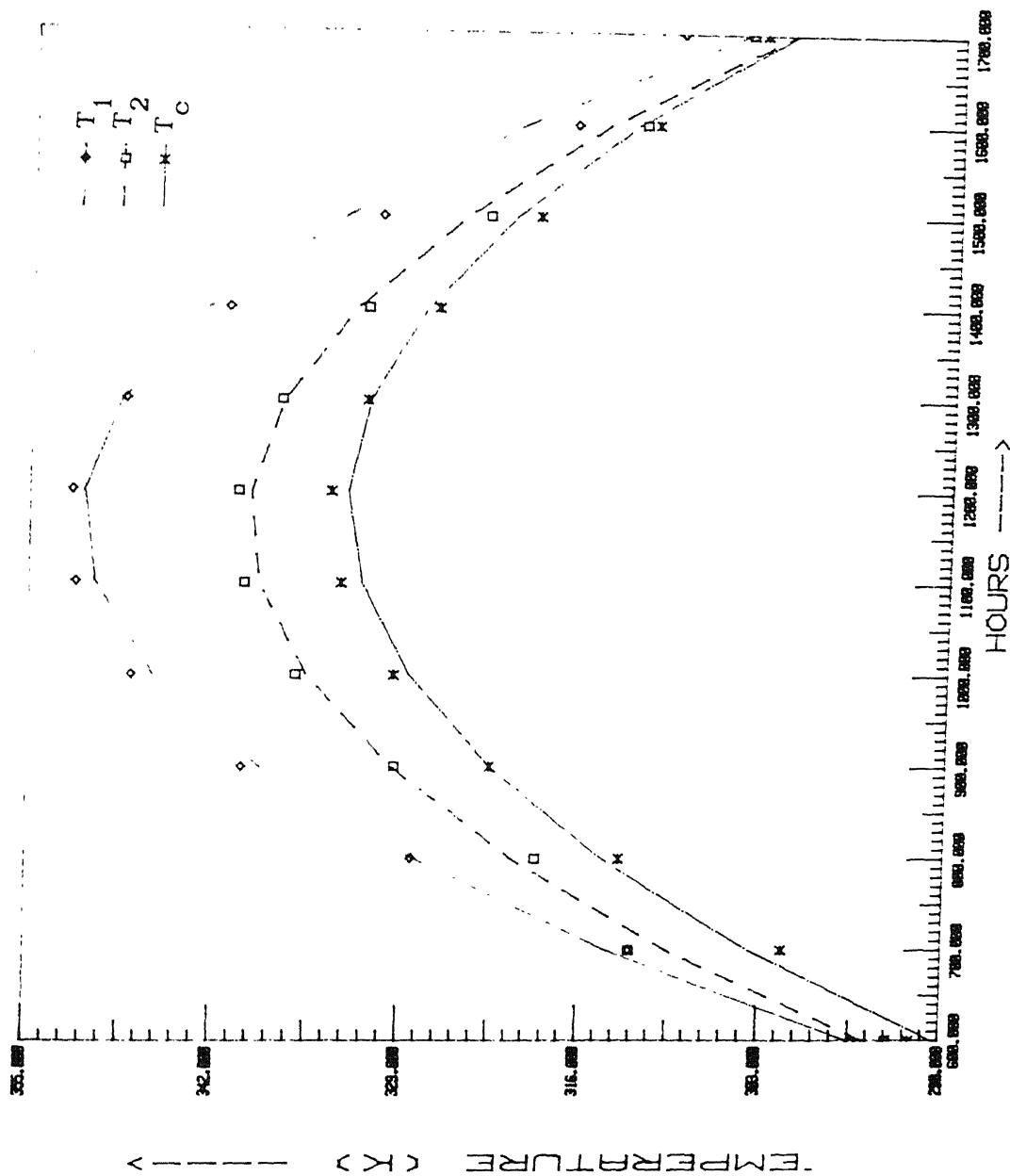


Fig.3.6b Hourly variation of temperatures of glass cover, intermediate glass plate and absorber plate

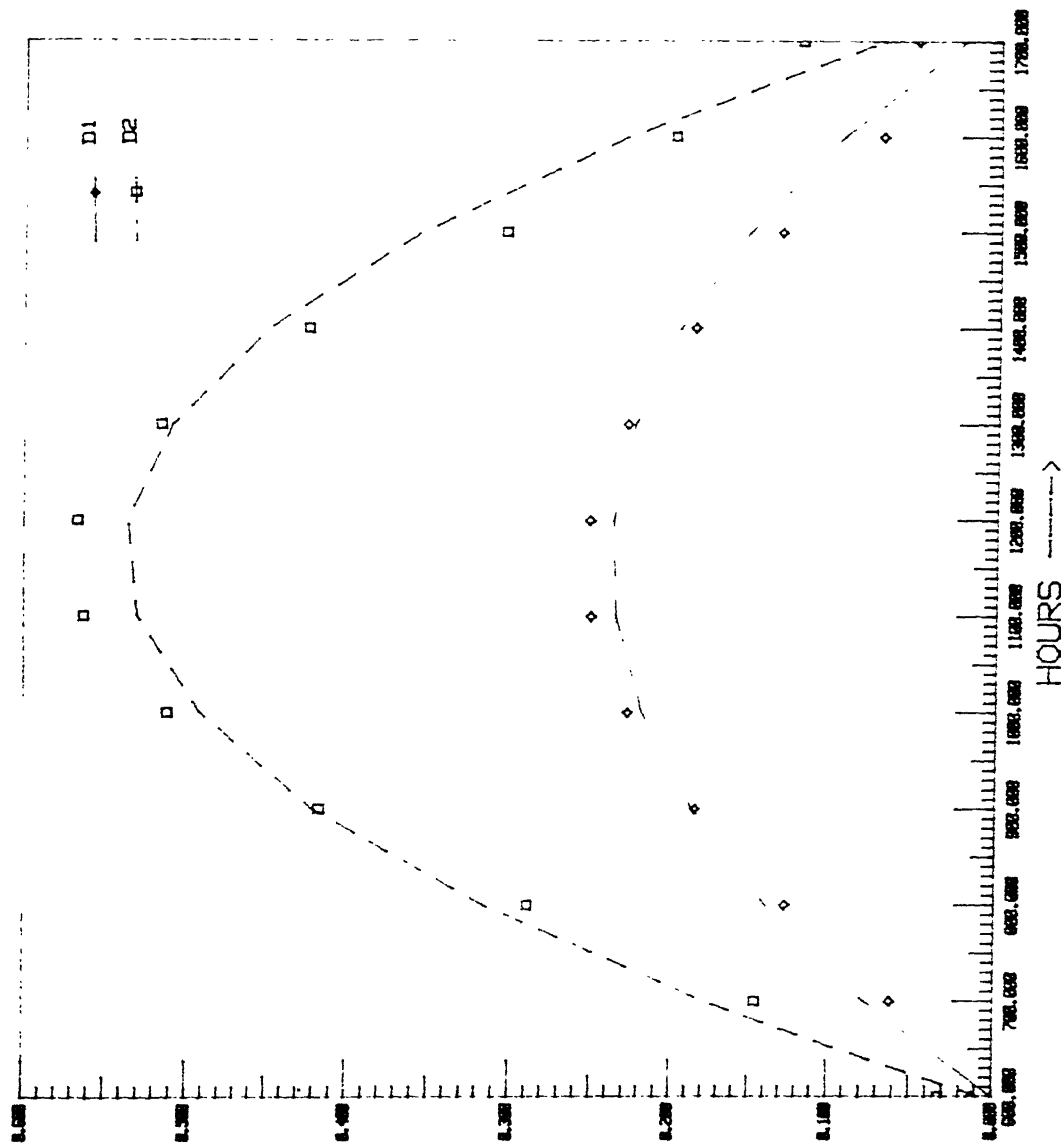


Fig.3.6c Hourly variation of distillate output

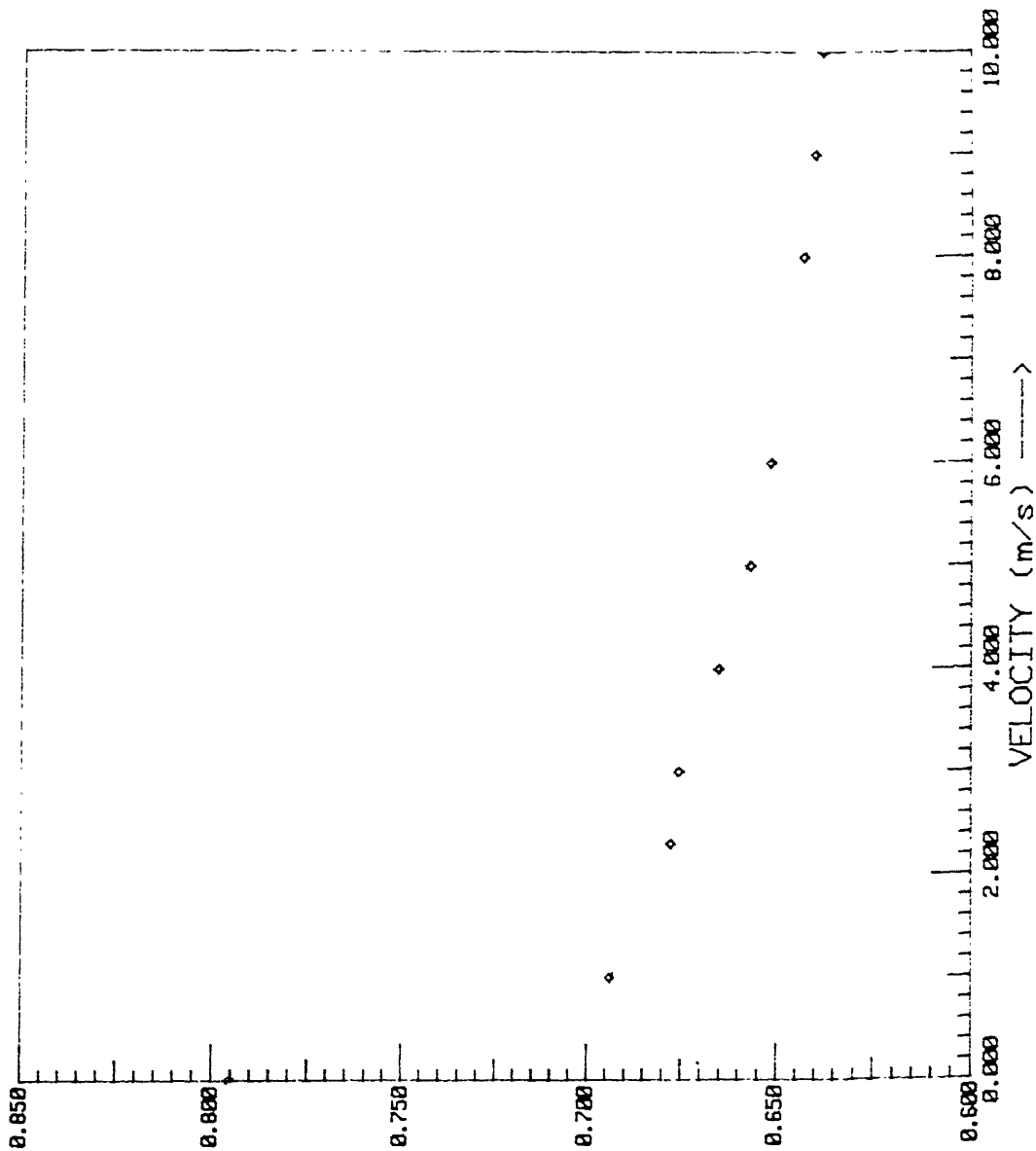


Fig.3.7 Effect of ambient air velocity on distillate output

Fig. 3.8 plots the effect of inlet water temperature on the distillate output for a double-effect solar still. There is a net increase in the net distillate output due to the increased temperature of the inlet water to the lower stage of the solar still. This is quite obvious from the fact that the amount of energy required for the evaporation of the saline water decreases as the inlet saline water temperature increases.

Fig 3.9 shows the effect of reduced operating pressure on the distillate output of the double-effect still. It can be seen that as the operating pressure is reduced the net distillate increases. It is apparently due to the fact that at a lower operating pressure the water evaporates at a much lower temperature thereby resulting in higher water mass being evaporated.

Fig. 3.10 shows the variation of distillate output with mass flow rate of saline water in the lower stage of the double-effect solar still. The distillate output falls as the mass flow rate is increased. This is due to the fact that the increased flow rate in the lower stage would take away some of the incoming heat, thereby resulting in the lowering of the absorber plate temperature and the subsequent decrease of the distillate output.

3.3 CONCLUSIONS

From the results of the present study, the following inferences may be drawn:

- a. A double-effect solar still is about 35 to 40 percent more efficient than a single-effect still.

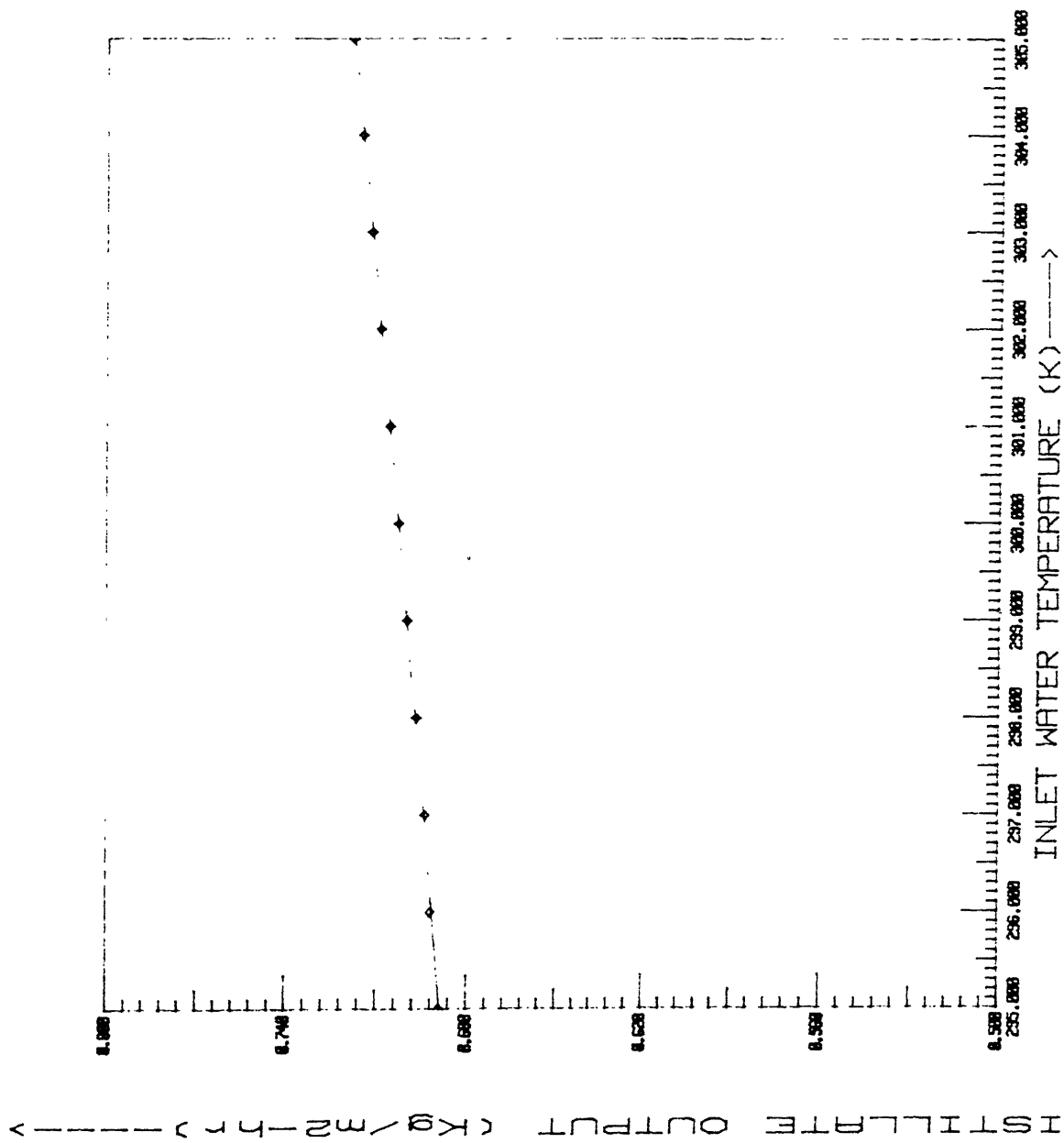


Fig. 3.8 Effect of inlet water temperature on distillate output

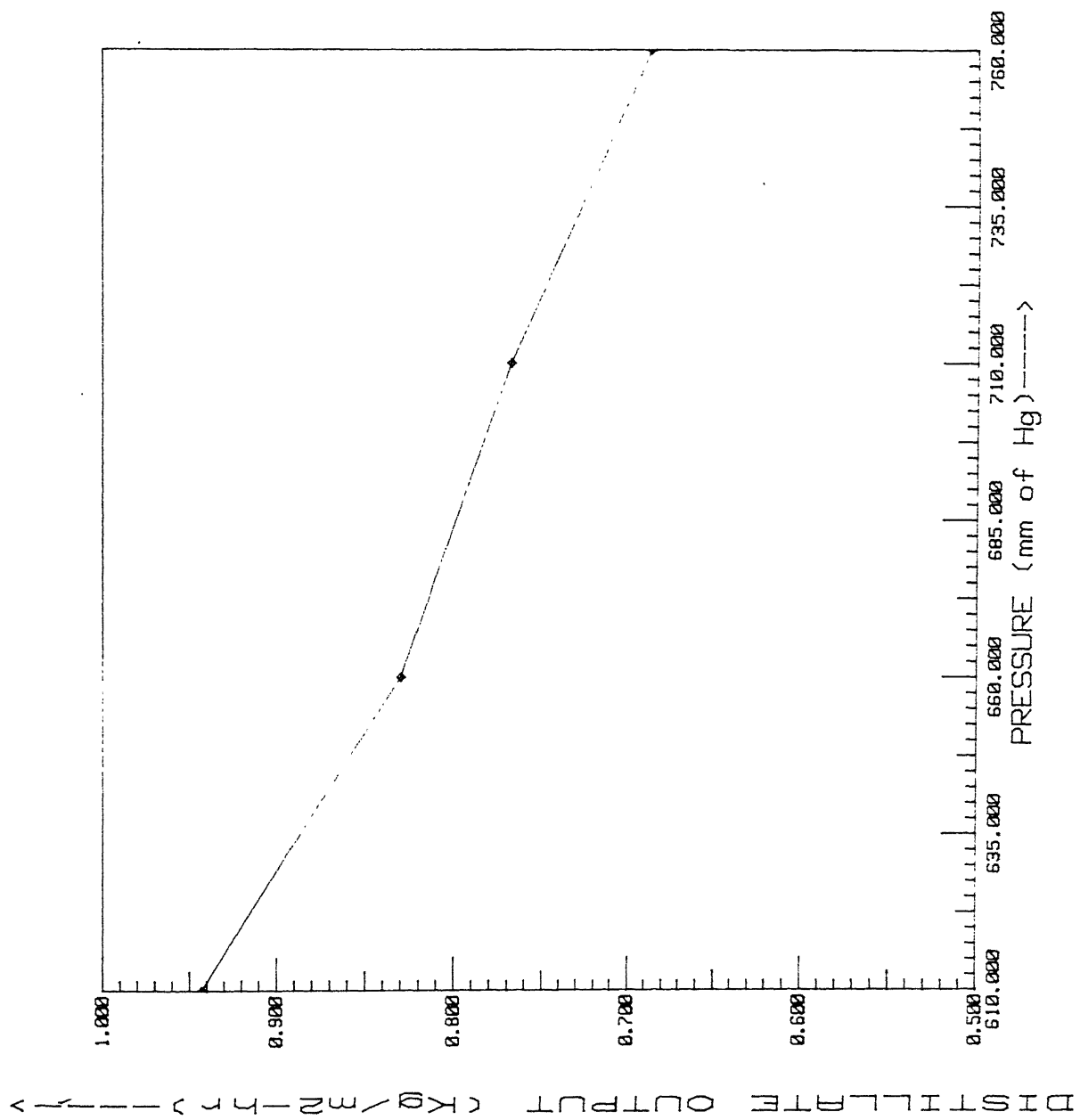


Fig.3.9 Effect of operating pressure on distillate output

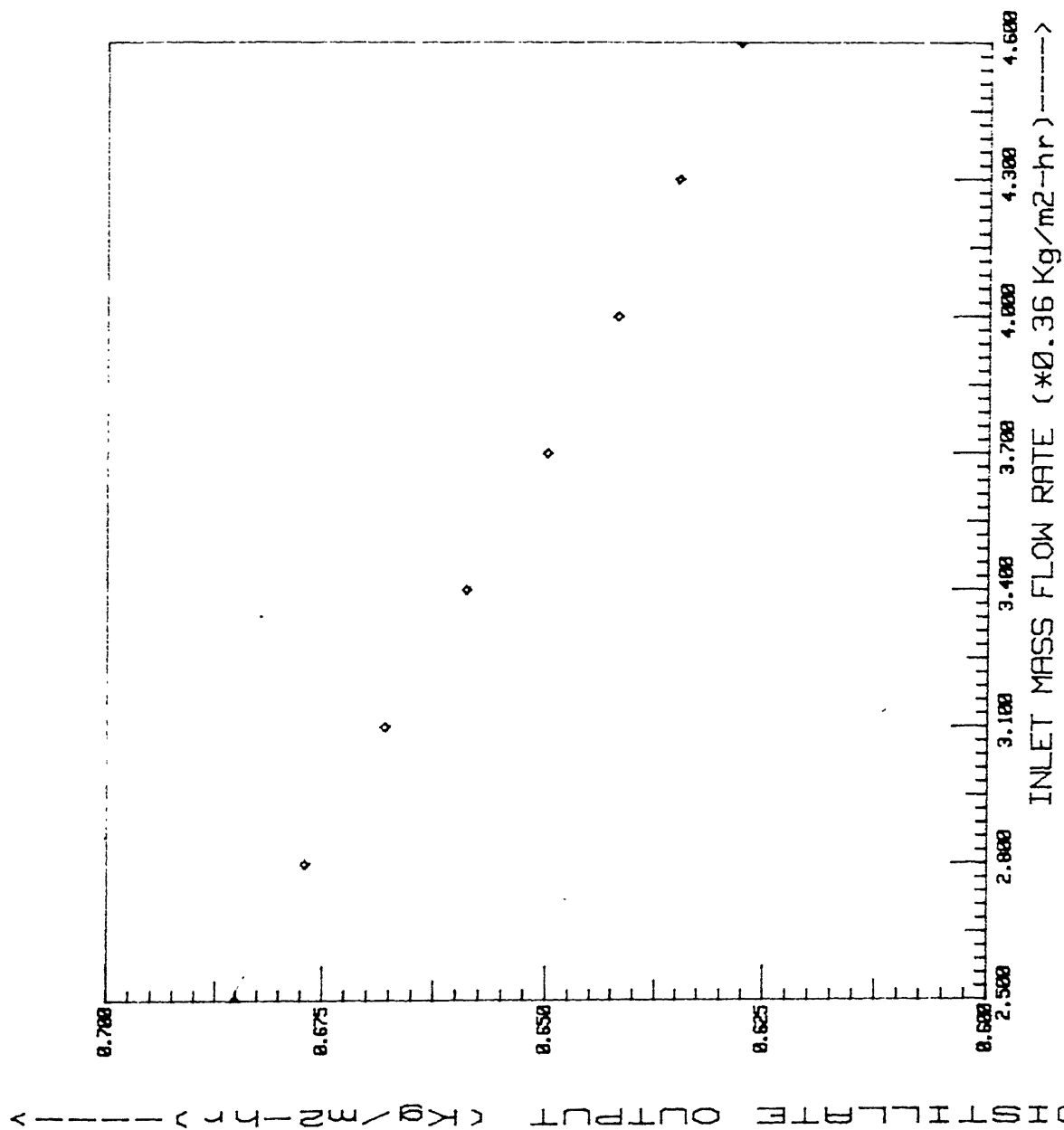


Fig.3.10 Effect of mass flow rate in lower stage on distillate output

- b. The net distillate output for a double-effect still varies from $0.403 \text{ Kg/m}^2 \text{ hr}$ to $0.886 \text{ Kg/m}^2 \text{ hr}$ for various months of the year.
- c. The still has to be operated at the optimal mass flow rate corresponding to given still design conditions to achieve higher levels of efficiency. This mass flow rate should be such as to almost equal the distillate output for the particular month.
- d. Efficiency of the still increases with rise in inlet water temperature. This fact helps us to use the hot waste water from various thermal plants for the still. It is quite convenient to have an inlet water temperature of 303 K for the improved performance of the still.

3.4 SUGGESTIONS FOR FUTURE WORK

The present study is basically a theoretical investigation into the performance of a double-effect solar still. The next logical step towards the extension of the present work would be to construct and study an experimental double-effect still to verify the theoretical results obtained in this study under actual conditions.

REFERENCES

1. A. MANI, Handbook of solar radiation data for India
2. M.P.AGARWAL, Solar Energy, S.Chand and Company Ltd., New Delhi
3. KARL W. BOER, Advances in Solar Energy Vol.4, American Solar Energy Society, Inc. (1983)
4. M.A.S. MALIK, G.N. TEWARI, A.KUMAR and M.S. SODHA, Solar Distillation, Pergamon Press, London (1982)
5. J.A. DUFFIE and W.A.BECKMAN, Solar Engineering of Thermal Processes, Wiley, New York, NY(1980)
6. A.A.M. SAYIGH, Solar Energy Engineering, Academic Press, New York(1977)
7. F.P. INCROPERA and D.P. DEWITT, Fundamentals of Heat Transfer Wiley, New York, NY(1981)
8. G. FRICK and J.V. SOMMERFIELD, Solar Stills of Inclined Evaporating Cloth, Solar Energy 14, 427(1973)
9. S.M.A. MOUSTAFA and G.H. BRUSEWITZ, Direct use of solar energy for water desalination, Solar Energy 22, 141(1979)
10. H.C. BRYANT and I. COLBECK, Solar Energy Transmission through water layer, Solar Energy 19, 321(1975)
11. A. RABL and C.E. NIELSEN, Empirical Correlation equation for Solar Radiation Transmission through water layer, Solar Energy 17, 1(1975)
12. M.S. SODHA, J.K. NAYAK, G.N. TEWARI AND A.KUMAR, Double basin solar stills, Energy Conversion Management 20, 23(1980)
13. G.N. TEWARI, Demonstration Plant of a Multi-Wick Solar Still, Energy Conversion Management 24, 313(1984)
14. S.N. RAI and G.N. TEWARI, Single basin solar still coupled with flat plate collector, Energy Conversion Management 23, 145(1982)
15. H.M. YEH, Effects of Climatic, Design and Operational parameters on air humidity at inside cover surface of basin type solar distillers, Energy 8, 839(1983)
16. Y.P YADAV and G.N. TEWARI, Analytical model of a solarium for cold climate, Energy Conversion Management 28, 8(1988)

17. G.N. TEWARI, S.P GUPTA and S.A. LAWRENCE, Transient analysis of solar still in presence of dye, Energy Conversion Management 29, 59(1989)
18. H.M. YEH and L.C. CHEN, Basin type solar distillation with air flow through a still, Energy 10, 1237(1985)
19. H.M. YEH, L.W. TEN and L.C. CHEN, Basin type solar distillers with operating pressure reduced for improved performance, Energy 10, 683(1985)
20. P.T. TSILINGRIS, An accurate upper estimate for transmission of solar radiation, Solar Energy 40,41 (1988)
21. B. PALANCZ, Analysis of solar dehumidification drying, Int. J. Heat Mass Transfer 27, 647(1984)
22. Y.P. YADAV and K.JHA, A double basin solar still coupled to a collector and operating in thermosiphon mode, Energy 14, 653(1989)
23. S.W. CHURCHILL and H.S. CHU, Correlation equations for laminar and turbulent free convection from a vertical plate, INT. J. Heat Mass Transfer 18, 1323(1975)
24. A. KUMAR, M. SINGH and J.D. ANAND, Transient performance of a double basin solar still integrated with a heat exchanger, Energy 14, 643(1989)
25. P.I. COOPER, Digital simulation of solar still processes, Solar Energy 12, 3 (1969)
26. A. MOUCHOT, The Solar Heat And Its Industrial Applications, Paris (1969)
27. C.G. ABBOT, The Sun And Welfare Of Man, Smithsonian Scientific Series
28. G. FRICK and J.V. SOMMERFIELD, Theory and experience with experimental still in Chile, Solar Energy 14,4 (1973)
29. G. NEBBIA and G. MENOZZI, Proceedings International Symposium, Milano, 129 - 132 (1966)

```

*****
*
*       APPENDIX A
*
*****

```

```

-----*
c  THIS PROGRAM USES THE SUBROUTINE COSNBF FROM THE NAG LIBRARY TO SOLVE*
c  THE ENERGY BALANCE EQUATIONS FOR THE DOUBLE-EFFECT SOLAR STILL AND*
c  CALCULATES THE TEMPERATURES OF COVER, INTERMEDIATE GLASS PLATE AND*
c  ABSORBER PLATE FOR MONTHLY DATA FOR SOLAR RADIATION. IT ALSO CALCULATES*
c  THE NET DISTILLATE PRODUCTION RATE FOR VARIOUS MONTHS.
-----*

```

```

program soletill
implicit double precision (A - Z)
EXTERNAL X02AJF
EXTERNAL COSNBF,fcu
integer n,lwa
parameter (n=3,LWA = n*(3*n+13)/2)
common /const1/Ab,As,At,ATa,PT,Ti,W,L,p,v,H, AI0,Aphi
common /const2/Asphi,AD1,AD2
common /const3/C+2,CFc,n1,ha,h2t,RA1,RA2s,RA2t,h2s
common /const4/Acosphi,Asinphi
common /const5/ IFAIL
integer i,NO,IFAIL,IFLAG
dimension I(3),fvec(n),WA(LWA)
INTRINSIC SORT,dble
character datafile *3
character datafil1 *3
character datafil2 *3

write(*,('No of input files >> ','$'))
read(*,*)NO
write(*,('Name of the output data file >> ','$'))
read(*,('A3'))datafil1
open (unit=22,file='results/' //datafil1)
write(*,('Name of output files >> ','$'))
read(*,('A3'))datafil2
open (unit=20,file='plot_results/' //datafil2)
do j =1, NO
write(*,('Name of the input data file >> ','$'))
read(*,('A3'))datafile
open (unit=21,file=datafile)
call readvar
write(20,*) '12', ' 6'
do i=1,12
read(21,*) AI0,ATa,Aphi
call initialise(Acosphi,Asinphi)
Ti=ATa - 4
I(1)= ATa+10
I(2)= ATa+5
I(3)= ATa+3
IFAIL = 0
TOL = SQRT(X02AJF())
TOL = 1d-3
call COSNBF(fcu,n,T,fvec,TOL,WA,LWA,IFAIL)
write(22,999) i,T(1),T(2),T(3),AD1*36000,AD2*36000
1 write(20,*) i,T(1),T(2),T(3),AD1*36000,AD2*36000,(AD1+AD2)*36000
end do
close(unit=21)
end do
close(unit=22)
close(unit=20)
stop
FORMAT(' Temperature Calculations for Month ',I2,'//5X','T1 = ',F7.3,

```

CEP 114835

```

1  ' T2 = ',F7.3,' Tc = ',F7.3,/5x,' D1 = ',F5.3,2X,' D2 = ',F5.3,
2  ' n=',F5.3/)
    end
    subroutine fcn(n,T,fvec,IFLAG)
c -----*
c  THIS IS THE EXTERNAL SUBROUTINE WHICH NEEDS TO BE PROVIDED TO THE*
c  SUBROUTINE COSNBF FROM THE NAG LIBRARY. THIS SUBROUTINE CONTAINS THE*
c  VARIOUS EQUATIONS IN THE FORM OF NON-LINEAR FUNCTIONS AND CALCULATES*
c  THEIR VALUES TO BE FED TO COSNBF TO OBTAIN A CONVERGING SOLUTION TO*
c  THE GIVEN EQUATIONS.
c -----*
    implicit double precision (A - Z)
    common /const1/Ab,As,At,ATa,PT,Ti,W,L,p,v,H, AI0,Aphi
    common /const2/Asphi,AD1,AD2
    common /const3/CF2,CFc,h1,ha,h2t,RA1,RA2s,RA2t,h2s
    common /const5/ IFAIL
    integer IFAIL,IFAIL,n
    dimension I(3),fvec(n)

    I1=I(1)
    I2=I(2)
    Ic=I(3)

    if(T2 LT Tc) T2 = Tc
    if(T1 LT T2) T1 = T2

    call calpard(T1,T2,Tc)

    AD1=2.59+h1*((fps(T1)/(PT-fps(T1)))
1      -CF2*fps(T2)/(PT-CF2*fps(T2)))

    AD2=2.59+((h2t*At+h2s*As)/Ab)*(fps(T2)/(PT-fps(T2))-CFc*
1      fps(Ic)/(PT-CF2*fps(Tc)))

    call calparf(T1,T2,Tc,qe2,qc2,qn2,qca,qra,qe1,qc1,qn1,tw,Lw)

    fvec(1)=0.12*AI0+qe2+qc2+qn2-qca-qra
    fvec(2)=(0.85*AI0)*Lw+(0.102*AI0)*tw+(3.0d-5)*(Ti-Tc)+qe1+
1      qc1+qn1-((3.0d-5)-AD2)*(T2-Tc)-AD1*(T2-Tc)-qe2-qc2-qn2
    fvec(3)=0.7825*AI0*tw+(2.5d-5)*(Ti-Tc)-qe1-qc1-qn1
1      -((2.5d-5)-AD1)*(T1-Tc)

    if(IFAIL.leq 4) then
        fvec(1) = 0.0
        fvec(2) = 0.0
        fvec(3) = 0.0
    endif
    return
end

subroutine calparf(T1,T2,Tc,qe2,qc2,qn2,qca,qra,qe1,qc1,qn1,tw,Lw)
c -----*
c  THIS SUBROUTINE CALCULATES THE TOTAL HEAT FLUX CONTRIBUTION DUE TO*
c  CONVECTION, RADIATION AND EVAPORATION SEPARATELY. THIS UTILISES THE*
c  HEAT TRANSFER COEFFICIENT VALUES CALCULATED FROM SUBROUTINE CALPARD*
c  AND STILL DESIGN PARAMETERS FROM INPUT FILE.
c -----*
    implicit double precision (A - Z)
    common /const1/Ab,As,At,ATa,PT,Ti,W,L,p,v,H, AI0,Aphi
    common /const2/Asphi,AD1,AD2
    common /const3/CF2,CFc,h1,ha,h2t,RA1,RA2s,RA2t,h2s
    qe2=L(T2)*AD2
    qc2=(h2t*At+h2s*As)*(T2-Tc)/Ab
    qn2=0.9*(1.36d-12)*((T2)**4-(Tc)**4)

```

```

      qca=ha*(Tc-Ata)
      qra=0.95*(1.36d-12)*((Tc)**4-(Ata)**4)
      qe1=L(T1)*AD1
      qc1=h1*(T1-T2)
      qr1=0.96*(1.36d-12)*((T1)**4-(T2)**4)
      tw=(0.732-0.056*((p+0.0084)/p)*log(p+0.0084)
      - (0.0084/p)*(log(0.0084)-1))
1      lw=1-tw
      return
      end

      subroutine initialise(Acosphi,Asinphi)
c -----*
c THIS SUBROUTINE CALCULATES THE VARIOUS SINE AND COSINE VALUES OF THE*
c STILL INCLINATION ANGLE AND ALSO THE AREAS OF STILL AND WATER SURFACE*
c IT USES THE INPUTS SUCH AS STILL INCLINATION ANGLE AND STILL DESIGN*
c PARAMETERS*
c -----*
      implicit double precision (A - Z)
      common /const1/Ab,As,At,ATa,PT,Ti,W,L,p,v,H, AI0,Aphi
      common /const2/Asphi,AD1,AD2
      common /const3/CF2,CFc,h1,ha,h2t,RA1,RA2s,RA2t,h2s
      pi = 22/7
      Aphi = Aphi + pi/180.0
      Acosphi=dcos(Aphi)
      Asphi =dsin(Aphi)
      Asinphi=(dsin(1.8+Aphi))*1.6
      Ab=W*L
      As=(Ab+Asphi)/Acosphi
      At=Ab/Acosphi
      return
      end
      subroutine readvar
c -----*
c THIS SUBROUTINE READS THE VALUES OF INPUT PARAMETERS FROM THE INPUT FILE*
c AND SUPPLIES THEM FOR CALCULATIONS IN VARIOUS OTHER SUBROUTINES.*
c -----*
      implicit double precision (A - Z)
      common /const1/Ab,As,At,ATa,PT,Ti,W,L,p,v,H, AI0,Aphi
      common /const2/Asphi,AD1,AD2
      common /const3/CF2,CFc,h1,ha,h2t,RA1,RA2s,RA2t,h2s
      read(21,*) W,L,H,p
      read(21,*) PT,v
      return
      end
c -----*
      double precision      function fps(T)
      implicit double precision (A - Z)
      fps=739.4+18.717*T+3.1595*T*T-2.3025d-2*(T*T*T)
      +8.9819d-4*(T*T*T*T)*7.5d-3
      return
      end
c -----*
      double precision      function fplus(x)
      implicit double precision (A - Z)
      if (x.GT.0.0) then
        fplus=x
      else
        fplus=0
      endif
      return
      end
c -----*
      double precision      function Ka(T)
      implicit double precision (A - Z)
      Ka=(2.4172+7.580d-3*T)d-2

```



```

      return
end

```

```

c -----
      double precision      function R(T)
      implicit double precision (A - Z)
      R=(1.2923-4.514d-3*T+1.0583d-5*T*T)
      return
end

```

```

c -----
      double precision      function Ca(T)
      implicit double precision (A - Z)
      Ca=(1.00324+6.76d-5*T)d3
      return
end

```

```

c -----
      double precision      function nu(T)
      implicit double precision (A - Z)
      nu=0.1d-3*(4.0201+0.74582*T-0.00057171*(T**2)
1      +(2.9928d-7)*(T*T*T)-(6.2524d-11)*(T**4))
      return
end

```

```

c -----
      double precision      function L(T)
      implicit double precision (A - Z)
      L=(2500.2-2.2975*T-1.3105d-3*T*T)d3
      return
end

```

```

c -----
c THIS SUBROUTINE CALCULATES THE VALUES OF VARIOUS HEAT TRANSFER COEFFICIENTS
c AND RAYLEIGH NUMBERS WHICH ARE REQUIRED FOR VARIOUS HEAT TRANSFER TERMS
c IN THE FUNCTIONS IN FCN
c -----

```

```

      subroutine calpard(T1,T2,Tc)
      implicit double precision (A - Z)
      common /const1/Ab,As,At,ATa,PT,Ti,W,L,p,v,H, AI0,Aphi
      common /const2/Asphi,AD1,AD2
      common /const3/CF2,CFc,hf,ha,h2t,RA1,RA2s,RA2t,h2s
      common /const4/Acosphi,Asinphi
      CF2=0.512*(((T1-T2)/H)**0.273)
      CFc=0.606*(((T2-Tc)/H)**0.119)
      RA2t=(2+981*(H*H*H)*R(T2)*C(T2)/(nu(T2)*Ka(T2)*(T2+Tc)))*
1      ((T2-Tc)+((fps(T2)-CFc*fps(Tc))/(2.65*PT-fps(T2)))*(T2-273.0))
      RA1=(2+981*(H*H*H)*R(T1)*C(T1)/(nu(T1)*Ka(T1)*(T1+T2)))*
1      ((T1-T2)+((fps(T1)-CF2*fps(T2))/(2.65*PT-fps(T1)))*(T1-273.0))
      RA2s=2*981+Acosphi*(p*p*p)*R(T2)*C(T2)*(T2-Tc)
1      /(nu(T2)*Ka(T2)*(T2+Tc))
      ha=(2.39d-5)*(5.7+3.8*v)
      h2s=(Ka(T2)/p)*(0.68+(0.67*RA2s**(1/4)))/
1      (1+1.703*(9/16))**(4/9)
      hf=(Ka(T1)/H)*(1+1.44*fplus(1-(1708/(RA1*Acosphi))))
1      *(1-1708*Asinphi/(RA1*Acosphi))
2      +fplus((RA1*Acosphi/5830)**(1/3)-1))
      h2t=(Ka(T2)/H)*(1+1.44*fplus(1-(1708/(RA2t*Acosphi))))*
1      (1-1708*Asinphi/(RA2t*Acosphi))
2      +fplus((RA2t*Acosphi/5830)**(1/3)-1))
      return
end
c -----

```

APPENDIX - B

CURVE FITTING AND METHOD OF LEAST SQUARES

Let (x_i, y_i) ; $i=1,2,\dots,n$ be a given set of n pairs of values X being independent variable and Y the dependent variable. The general problem in curve fitting is to find, if possible, an analytic expression of the form $y = f(x)$, for the functional relationship suggested by the given data.

If $Y = a_0 + a_1 X + a_2 X^2 + \dots + a_k X^k$ is the K^{th} degree polynomial of best fit to the set of points (x_i, y_i) $i=1,2,\dots,n$ the constants $a_0, a_1, a_2, \dots, a_k$ are to be obtained so that

$$E = \sum_{i=1}^n (y_i - a_0 - a_1 x_i - a_2 x_i^2 - \dots - a_k x_i^k)^2$$

is minimum.

Thus the normal equations for estimating $a_0, a_1, a_2, \dots, a_k$ are obtained on equating to zero the partial derivatives of E w.r.t. $a_0, a_1, a_2, \dots, a_k$ separately i.e.

$$\begin{aligned} \sum y_i &= na_0 + a_1 \sum x_i + \dots + a_k \sum x_i^k \\ \sum x_i y_i &= a_0 \sum x_i + a_1 \sum x_i^2 + \dots + a_k \sum x_i^{k+1} \\ &\dots\dots\dots \\ &\dots\dots\dots \\ \sum x_i^k y_i &= a_0 \sum x_i^k + a_1 \sum x_i^{k+1} + \dots + a_k \sum x_i^{2k} \end{aligned}$$

summation extending over i from 1 to n . These are $(K + 1)$ equations in $(K + 1)$ unknowns $a_0, a_1, a_2, \dots, a_k$ and can be solved algebraically.

THERMOPHYSICAL PROPERTIES OF WATER AND AIR

To analyze the effects of various parameters on the water production from a solar still, the model involves the use of accurate relations for the thermophysical properties of air and water. Using the Least-Squares method described previously the following relations for the thermophysical properties of air and water have been found to fit the data available from the literature[1] in the range $10 < T^{\circ}\text{C} < 100$ with a maximum error of 0.05 percent.

a. Density of air

$$\rho_a = 1.2923 - 4.514 \times 10^{-3} \times T + 1.0583 \times 10^{-5} \times T^2$$

b. Thermal conductivity of air

$$K_a = (2.4172 + 7.580 \times 10^{-3} \times T) \times 10^{-2}$$

c. Dynamic viscosity of air

$$\mu_a = (1.7205 + 4.564 \times 10^{-3} \times T) \times 10^{-5}$$

d. Specific heat capacity of air

$$C_{p_a} = (1.00324 + 6.76 \times 10^{-5} \times T) \times 10^3$$

e. Specific heat capacity of water

$$C_{p_w} = (4.197 - 8.699 \times 10^{-4} \times T + 3.686 \times 10^{-6} \times T^2) \times 10^3$$

f. Saturated vapor pressure of water vapor

$$P_v = 739.4 + 18.717 \times T + 3.1595 \times T^2 - 2.3025 \times 10^{-2} \times T^3 + 8.9819 \times 10^{-4} \times T^4$$

g. Latent heat of vaporization

$$\lambda_w = 2500.2 - 2.2975 \times T - 1.3105 \times 10^{-3} \times T^2) \times 10^3$$